



**HAL**  
open science

# Efficient utilization of hybrid photovoltaic/thermal solar systems by nanofluid-based spectral beam splitting: A review

Yue Jiao, Meibo Xing, Patrice Estellé

## ► To cite this version:

Yue Jiao, Meibo Xing, Patrice Estellé. Efficient utilization of hybrid photovoltaic/thermal solar systems by nanofluid-based spectral beam splitting: A review. *Solar Energy Materials and Solar Cells*, 2024, 265, pp.112648. 10.1016/j.solmat.2023.112648 . hal-04321539

**HAL Id: hal-04321539**

**<https://hal.science/hal-04321539v1>**

Submitted on 4 Dec 2023

**HAL** is a multi-disciplinary open access archive for the deposit and dissemination of scientific research documents, whether they are published or not. The documents may come from teaching and research institutions in France or abroad, or from public or private research centers.

L'archive ouverte pluridisciplinaire **HAL**, est destinée au dépôt et à la diffusion de documents scientifiques de niveau recherche, publiés ou non, émanant des établissements d'enseignement et de recherche français ou étrangers, des laboratoires publics ou privés.

# Efficient utilization of hybrid photovoltaic/thermal solar systems by nanofluid-based spectral beam splitting: A review

Yue Jiao<sup>a</sup>, Meibo Xing<sup>a,\*</sup>, Patrice Estellé<sup>b,\*</sup>

a. Beijing Engineering Research Center of Sustainable Energy and Buildings, School of Environment and Energy Engineering, Beijing University of Civil Engineering and

Architecture, Beijing, 100044, P. R. China

b. Univ Rennes, LGCGM, Rennes, 35000, France

## Abstract

Nanofluid-based spectral beam splitting (SBS) hybrid photovoltaic/thermal (PV/T) systems are a promising and efficient way to achieve full-spectrum utilization of solar energy. It utilizes the spectrum above bandgap of PV cells for power generation and the other sunlight for thermal output, decoupling PV and PT while having high total conversion efficiency. In this work, it is presented the opportunities and unique advantages of nanofluids in the field for SBS. The required properties of nanofluids as solar spectrum splitter, namely dispersion stability, thermal and optical properties are summarized. Furthermore, recent advances in SBS applications for PV/T systems are highlighted based on the classification of nanomaterials (metal, metal oxide, carbon-based as well as core@shell structures of metal and metal oxide composites). Finally, cost-effective analysis of nanofluid-based SBS applications is provided. Although efficiency has increased substantially and applications are promising, the issues of nanofluid stability under high solar radiation, full spectral matching and imperfect

---

\* Corresponding author. Tel/Fax: +86-29-82668725. Email: xingmeibo@bucea.edu.cn

\* Corresponding author. Email: patrice.estelle@univ-rennes.fr

economic analysis still need to be addressed for the wide application of SBS in PV/T systems. Finally, nanofluid-based SBS is one of the most prospective approaches to achieve efficient utilization of the full solar spectrum.

*Keywords:* Spectral beam splitting; Nanofluid; Solar energy; PV/T; Full-spectrum.

## 1. Introduction

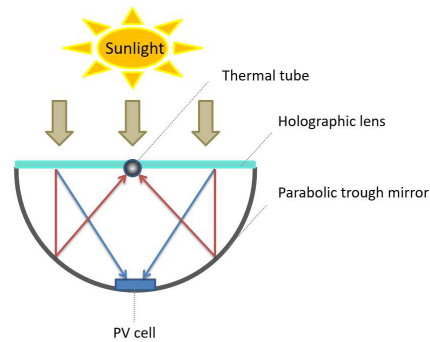
Solar energy is one of ideal replaceable sources for non-renewable energy sources, which is abundantly present and reaches the earth in various forms such as heat and light [1]. The utilization technologies of solar energy mainly include photovoltaic (PV), photothermal (PT), photochemistry and photobiology. The PV technology consists to absorb solar energy and convert it to electrical energy by PV modules. PV cells are wavelength dependent, and their spectral response is related to the bandgap of the semiconducting material itself. Therefore, only incident photons with energy greater than the bandgap energy of PV semiconductor materials can be excited to produce photovoltaic effect in the full spectrum solar radiation energy, while the energy of most of the remaining photons will be converted into thermal energy. As a result, the operating temperature of the cell will raise, which greatly reduce the open-circuit voltage and further degenerate the performance of PV modules. At the same time, the service life of PV cells will also be shortened due to long-term work under high temperature conditions [2]. Thus, the photovoltaic/thermal (PV/T) technology was developed to recovery the waste heat of cells for reducing the high temperature of PV modules and achieving higher total energy conversion efficiency [3].

Nevertheless, the temperature of the thermal collector is limited by the operating temperature of the PV cell due to the thermal energy is obtained from the recycling of the waste heat generated by the PV cell for the conventional PV/T system [4]. The spectral beam splitting (SBS) was proposed to enable PV and PT units to be performed separately by filtering the incident sunlight. Specifically, the solar radiation energy perfecting spectral response of the PV cell would directly incident to the PV modules for PV conversion, and other solar spectrum is used for PT conversion by using the SBS technology. The two units are arranged independently and work in parallel, realizing the decoupling of PV utilization and PT utilization temperature. According to the different principles of SBS, current methods mainly include liquid absorptive filter, solid film interference filter, holographic filter, luminescent filter and translucent PV cell with photon management. The methods and both their mechanisms and characteristics are gathered in Table 1.

Table 1 The SBS methods

Method	Diagram	Mechanism	Characteristics
Liquid absorptive filter		<p>The sunlight below bandgap energy of PV cell is highly absorbed by selective absorption liquid and the remaining radiation would highly transmit to reach the PV unit.</p>	<p>Advantages:                      (a) Avoiding the energy loss caused by secondary heat transfer.                      (b) Flexible deployment.                      (c) Cooling PV module first.</p> <p>Disadvantages:                      Requires spectral splitting liquid to be stable in the long-term.</p>
Solid film interference filter		<p>After mutual interference with sunlight, specific waveband reaches thermal unit through the film, and untransmitted part is highly reflected to PV cell.</p>	<p>Advantages:                      (a) Not absorbing sunlight natively.                      (b) Stable performance.</p> <p>Disadvantages:                      (a) Film fragility.                      (b) Fixed shape.                      (c) Vulnerable to the angle of sunlight.                      (d) Higher production cost.</p>

Holographic filter



The sunlight is partly transmitted to the PV cell through the holographic lens and partly combined with parabolic trough mirror which is then concentrated on heat pipe.

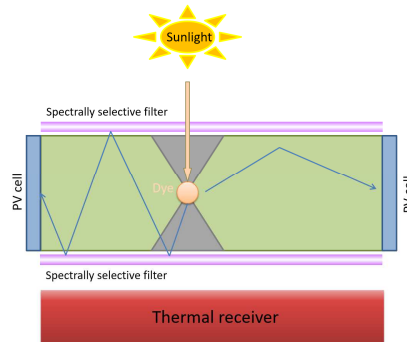
Advantages:

- (a) Not requiring complex tracking device.
- (b) Thin thickness.

Disadvantages:

Large area arrangement for application makes design complex and costly.

Luminescent filter



These dyes convert sunlight with energy exceeding band gap of PV cell into phosphorescence or fluorescence. Then luminescence produced by the Stokes shift is directed to the edge, where the PV cell is located. Meanwhile, the long-wave radiation passes through to heat absorber utilized.

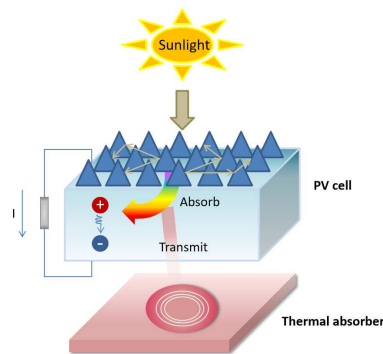
Advantages:

- (a) The cells are not directly exposed to the sun.
- (b) The heat absorber also receives heat generated by the Stokes transfer.

Disadvantages:

Relatively less efficient.

Translucent PV cell with photon management



A translucent PV cell with photon management is formed by using transparent conductive oxide placed on the back side of semiconductor material. The short wavelength sunlight is converted into electricity, and the long wavelength spectrum is passed to thermal absorber.

Advantages:

- (a) Reduced components.
- (b) No need to consider matching ability.

Disadvantages:

Higher costs.

Among the numerous SBS methods, liquid absorption filters are the most widely used because the spectral splitting liquid also acts as coolant [5]. The PV module would be cooled as it first passes the back of PV module and then flows to splitting device. The spectral splitting liquid can also store and transmit thermal energy, avoiding energy loss caused by secondary heat transfer. Since 2012 [6], the application of nanofluids for SBS in PV/T systems was increasingly studied as they can exhibit spectral splitting properties for excellent performance of PV/T systems because of their unique optical properties compared to conventional fluids. Furthermore, in contrast to most conventional liquids that can weakly absorb solar radiation, nanofluids only need a lower volume fraction of nanoparticles to exhibit high absorption properties and achieve large shifts in optical properties [7]. Meanwhile, the performance of the PV/T system using nanofluids can be optimized by varying the type, size, and concentration of nanoparticles, as well as the type of base fluid as well as the optical path length of filter. All these parameters can be flexibly adjusted to meet special needs and working environment in practical applications. The current review is intended to provide an up-to-date review on the investigation of nanofluid-based spectral splitting techniques in hybrid PV/T systems. Firstly, the interest of using nanofluids as spectral splitting liquid is introduced because of its hopeful matching of spectral response bandgap for the PV cells. Secondly, the required properties of nanofluids as spectral splitting liquid, such as stability, thermal and optical properties, are discussed. Then, the applications of different types of nanomaterials (metal, metal oxide, carbon-based as well as core@shell structures of metal and metal oxide composites) in PV/T systems is

summarized separately and cost analysis is performed, and challenges and perspectives in this field are finally presented.

## 2. Opportunities of nanofluids use for spectral beam splitting in PV/T systems

The solar spectrum contains wavelength range of 10-200 nm in far ultraviolet, 200-380 nm in near ultraviolet region, 380-760 nm in visible region, 760-3000 nm in near infrared region, and greater than 3000 nm in far infrared region, where the energy of far infrared, near infrared, visible, and ultraviolet are about 2.2%, 45.2%, 45.6%, and 7% respectively [8]. Fig.1 shows the solar spectrum distribution and spectral response of the various PV cells. The spectral response ranges of crystalline silicon (c-Si) solar cells, multicrystalline silicon (mc-Si) solar cells, copper indium gallium selenide (CIGS) thin film solar cells, gallium arsenide (GaAs) solar cells, cadmium telluride (CdTe) thin film solar cells, dye sensitized solar cells (DSC) and organic solar cells (OSC) are approximately 400-1100 nm, 400-1200 nm, 400-1100 nm, 400-900 nm, 400-850 nm, 400-750 nm, and 400-700 nm, respectively. For example, the threshold wavelength of crystalline silicon cell is approximately 400-1100 nm. That means only solar radiation with wavelength range of 400-1100 nm can be converted into electricity by crystalline silicon cells through photovoltaic effect, while the rest part of solar radiation can just be absorbed and converted into thermal energy. In addition, most of energy in the response band of crystalline silicon cells is less than the energy of solar radiation in this band, which means that a minority of energy can really be used and the remaining part will be transformed into thermalization energy [8]. The ideal spectral splitting liquid can transmit the response spectrum of cell to the PV for photoelectric conversion while



the rest of the spectrum are absorbed for photothermal conversion during SBS.

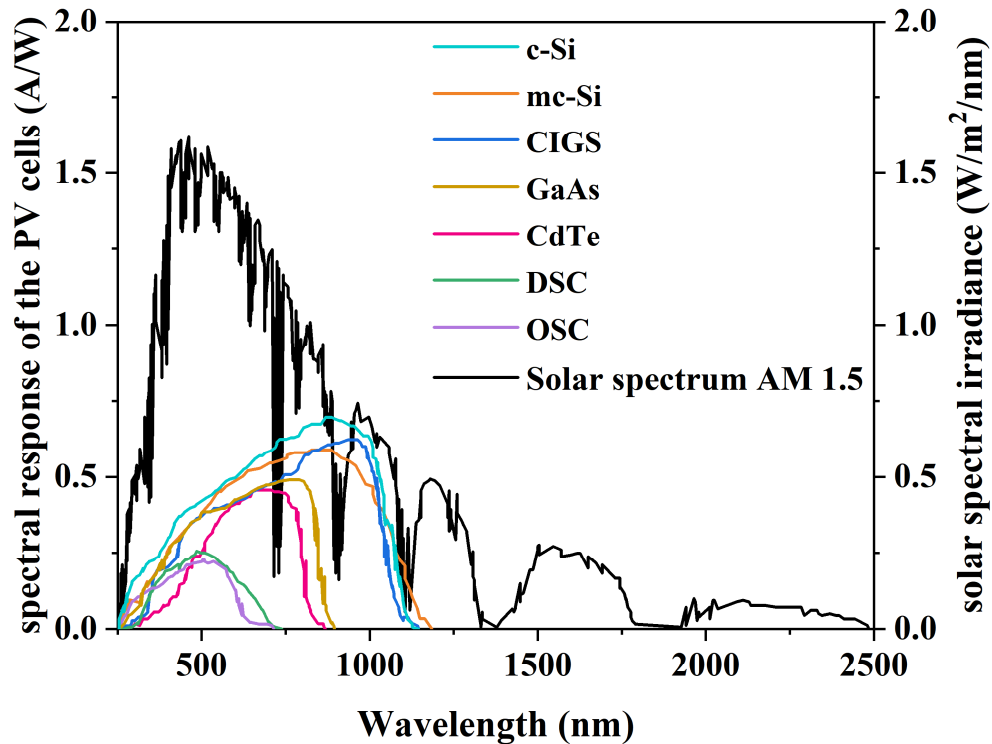


Fig. 1 The solar spectrum distribution and spectral response of various PV cells [9]

However, the absorption band of conventional spectral splitting liquids is fixed and mostly not coincident with the unresponsive band of PV cell. Therefore, the ideal spectral splitting liquid that can perfectly match spectral response bandgap of the PV cell are difficult to be found. Nanofluids are highly tunable, and it is expected to find matching working medium by adjusting the shape, size, concentration, type, base fluid, and so on [5,8], which means that the properties of nanofluids may be controlled by changing its various parameters. Some examples of how nanofluids can be used as spectral splitting liquids because of the presence of nanoparticles are given in the followings. The addition of  $\text{CoSO}_4$  salt solution to Ag/propylene glycol (PG) nanofluid would expand absorption range, which is 435-655nm. In this case nanofluid strongly

absorbs 350-615 nm and greater than 1420 nm wavelengths with high transmission at 615-970 nm, which basically coincides with spectral response band of 640-1080 nm for concentrated Si solar cells. The spectra required for concentrating Si cells are met by optical synergy between Ag nanoparticles and CoSO<sub>4</sub> salt solution [10]. Fe<sub>3</sub>O<sub>4</sub> nanoparticles absorb in 300-500 nm spectral region while copper sulphate (CS) absorbs strongly at 700 ~ 1000 nm. This allows Fe<sub>3</sub>O<sub>4</sub>/CS nanofluids to be used as filters for InGaP PV cells responding to 444-666 nm region [11]. By adjusting nanoparticle volume fraction, it is possible to tailor the required spectrum and optimize optical properties of filter. Nanofluids formed by suspending Ag@SiO<sub>2</sub> nanoparticles in PG solution can be used to match GaAs cells. Determining the optimum particle concentration and optical length leads to filtration efficiency exceeding 35% for GaAs cells [12]. By adjusting the type, concentration, shape of nanoparticles, type of base fluid, as well as the optical path length of filter, etc., absorbent nanofluids are obtained that meet the desired optical properties [5,8]. It is evidenced that the tunable selective spectral absorption characteristics of nanofluids can be used as a high-efficiency, compact and low-cost optical filtering for PV/T system.

### 3. Properties of nanofluids as solar spectrum splitters

As a crucial step in nanofluids usage as spectral splitting liquids, it is expected that nanofluids stay stable, e.g. that nanoparticles sedimentation is minimized with time. Also, among all thermophysical properties of nanofluids, both thermal and optical properties are of great interest for PV/T applications. As key parameters, dispersion stability, thermal and optical properties particularly influence the performance of

spectral splitting liquids. Hence, those properties are discussed in the following.

### *3.1 Dispersion stability*

The stability of nanoparticles dispersed in base fluid directly affects thermal and optical properties of nanofluids. Therefore, the preparation of uniformly dispersed stable nanofluids is essential and challenging. Current preparation methods include the one-step method in which nanoparticles are dispersed directly into base fluid for both preparation and dispersion, and the two-step method in which nanoparticles are synthesized first and then dispersed into desired base fluid for preparation. The Van der Waals force interactions between nanoparticles in this process can lead to self-aggregation phenomena [13]. The precipitation phenomena can also occur due to the difference in density between nanoparticles and the base solution. Besides, the morphology and nature of nanoparticles, particle and base fluid interaction, preparation process and technology all affect the nanofluid stability. At present, the ways to improve the dispersion stability of nanofluid include sonication, addition of surfactants, pH adjustment and surface modification technique by chemical treatment, as nively reviewed in [5,8,14].

The characterization used to assess the dispersion stability of nanofluids include the sedimentation observation method, UV-Visible spectrophotometry, zeta potential measurements and dynamic light scattering techniques. The comparison of these characterization methods is summarized in Table 2. The sedimentation observation method is used to judge the stability of nanofluids by observing the photos of their settling over a certain period of time. To improve the accuracy of results, it can only be

observed for a longer period of time, and quantitative results is not obtained. UV-Visible spectrophotometry is an effective method to capture the concentration variation in sedimentation of nanofluids by measuring absorbance of their upper solution based on the Lambert-Beer law. Baek et al. [14] used this method to compare the effect of two surfactants on the dispersion stability of 0.5%-alumina/distilled water nanofluid. The results indicated that the anionic surfactant could exhibit higher absorbance in the 650-1050 nm spectral range than the amphoteric surfactant and made alumina nanofluid more stable. The zeta potential measurement implies the strength of repulsion between nanoparticles. A higher zeta potential value represents a stronger repulsion between the particles. Nanofluids are assumed to possess good stability when the potential value is higher than 30mv [15]. The dynamic light scattering technique is determined by measuring the change in particle size distribution caused by agglomeration in diluted nanofluid suspensions that is suitable for high transparency and low concentration [16].

Long-term stability of nanofluids is a basic requirement and a key bottleneck for realizing industrial wide applications. The instability of nanofluids after long-term operation will lead to system performance degradation. Moreover, the stability level of nanofluids in actual operation is affected by external operating conditions such as confinement, high temperature and magnetic field. The real stability level situation of nanofluids will be reviewed. Primarily, precipitation and aggregation of nanoparticles from nanofluids in closed microchannels can occur, which can severely affect flow and heat transfer such that it increases the cost of pumping. Sarafraz et al. [17] investigated the level of performance of water-based graphene nanosheets in microchannels. It was

found that high particle concentrations and service periods lead to intense fouling generating greater thermal resistance and thermal performance improves at increased pressure drop and pumping.

High temperatures degrade the added surfactants and polymers, which has bad effect on the stability level of the nanofluids. Hordy et al. [18] investigated the stability of MWCNT nanofluids with base fluids of water, ethylene glycol, propylene glycol, and Therminol VP-1, respectively. All except Therminol VP-1/MWCNT nanofluids showed long-term stability of 8 months. In addition, the nanofluids were found to be less stable in high temperature environments by heating cycles at 220 °C. Tavares et al. [19] synthesized heat stabilized Cu/EG nanofluids without any surfactant. However, agglomeration still occurred at 197 °C. Sani et al. [20] prepared stabilized ethylene glycol-based single-walled carbon nanohorn nanofluids, which could remain stable for six months until the temperature reached 150 °C. Lin et al. [21] stated that nanofluids become unstable when changing from laminar to turbulent flow due to the difference in pressure drop and heat transfer between them. Nanofluids will also exhibit instability when leaving thermal equilibrium. Since the significant aggregation of nanofluids at high temperatures tends to be mostly irreversible. Hence, they should remain stable over a wide range of temperatures.

In the field of SBS, magnetic field-induced aggregation of nanoparticles can modulate the nanofluid absorption spectra, but also has crucial effects on the stability. Chang et al. [22] studied the effect of magnetic field induction on the stability of CuO nanofluids. Under the effect of magnetic field, the repulsive potential energy between

two suspended particles is weakened leading to increased aggregation of nanoparticles. The CuO nanofluid is destabilized faster under strong magnetic field and the sedimentation phenomenon is more obvious with longer time of action. However, the effect of magnetic permeability on CuO nanofluid is relatively minor. Wang et al. [23] pointed out that electrostatic or steric stabilization techniques are required in order to stabilize the nanofluid after removal of the magnetic field to ensure reusability.

Table 2 Characterization method for nanofluid stability evaluation

Method	Analysis results	Application conditions
Sedimentation observation	Qualitative	Low concentration
UV-Visible spectrophotometry	Quantitative	High transparency
Zeta potential	Qualitative	-
Dynamic light scattering	Quantitative	High transparency and low concentration

### 3.2 Thermal properties

Nanofluid can be used as the absorbing and heat transfer medium for PT conversion while acting as spectral splitting liquid, so the thermal properties of nanofluid have an impact on the total efficiency of PV/T system. In particular, thermal conductivity is the most important parameter, and the relevant studies about this property for spectral splitting nanofluids are summarized in Table 3. Yavari et al. [24] prepared water-based nanofluids of 0.1 wt% MWNT/Fe<sub>3</sub>O<sub>4</sub> and measured the thermal conductivity at different magnetic fields. The outcomes showed that the thermal conductivity was enhanced by 52% and 11.9% for the temperature gradient parallel and perpendicular to the magnetic field at the magnetic field strength  $H = 0.14$  T, respectively. A reduced graphene oxide-Fe<sub>3</sub>O<sub>4</sub> (rGO-Fe<sub>3</sub>O<sub>4</sub>) composite nanofluid was prepared by Barai et al. [25]. The thermal conductivity of rGO-Fe<sub>3</sub>O<sub>4</sub> nanofluid was increased by 41.35%, 57.23%, 66.76%, 77.72% and 83.44% at 40°C for 0.01, 0.05,

0.07, 0.1 and 0.2 vol% concentrations, respectively. Maheshwary et al. [26] investigated the effect of different shapes (spherical, cubic and rod) on the thermal conductivity of nanoparticles. Water-based nanofluids of CuO, MgO, TiO<sub>2</sub>, ZrO<sub>2</sub> and Al<sub>2</sub>O<sub>3</sub> were prepared in a two-step process. The results showed that the thermal conductivity of the cubic-shaped Al<sub>2</sub>O<sub>3</sub> nanofluid was 3.13 times higher than that of the base fluid when the concentration was 2.5 wt%. Simultaneously, the cubic-shaped nanoparticles have the highest enhanced thermal conductivity rate compared to spherical and rod-shaped nanoparticles. Xian et al. [27] prepared hybrid nanofluids by dispersing graphene nanosheets (GnPs) and titanium dioxide (TiO<sub>2</sub>). The thermal properties of the nanofluids were measured at concentrations of 0.1, 0.075, 0.05 and 0.025 wt% in the range of 30°C to 70°C. It was shown that the maximum thermal conductivity of the hybrid nanofluid at 0.1 wt% at 60°C increased by 23.74% and exhibited higher thermal conductivity than the mono nanofluid at all concentrations and temperature ranges from 30°C to 50°C. Oraon et al. [28] investigated the effect of increasing the weight percentage of hard magnetic Sm-Co-based nanoparticles on the thermal conductivity of silicone oil in the presence of an external magnetic field. The thermal conductivity of Sm-Co nanofluids with a mass fraction of 15 wt% was increased by approximately 373% when the magnetic flux density was 0.5 T. Pourrajab et al. [29] experimentally analyzed the synergistic effect on improving the thermal conductivity in water-based hybrid nanofluids mixed with MWCNTs and Ag nanoparticles. It was revealed that the thermal conductivity ratio of the hybrid nanofluid exhibited a nonlinear increase when the temperature and concentration were increased. And the thermal conductivity of the

hybrid nanofluid containing 0.04 vol% Ag nanoparticles and 0.16 vol% MWCNTs was synergistically increased by 47.3% compared to the normal water-based fluid. The thermal conductivity enhancement rate of nanofluids are different, which is caused by the selected nanoparticles and their concentrations, the type of base fluid, as well as the fluid temperature. In particular,  $\text{Fe}_3\text{O}_4$ , MWCNTS and graphene contribute considerably to the improvement of the thermal properties.

The heat transfer enhancement mechanism of nanofluids is quite complex compared with the conventional fluids. The following mechanisms [30, 31] are considered to be the main reasons for the thermal conductivity enhancement. (1) Brownian motion is the random motion of nanoparticles at the microscopic scale, which prevents the sinking of particles due to the influence of gravity. And the increase in thermal conductivity due to Brownian motion is negligible when the nanoparticle concentration is low or the diameter is very small. (2) Thermophoresis is a temperature gradient in a fluid that establishes convective flow, resulting in an increase in thermal conductivity caused by the directional flow of high temperature particles hitting low temperature particles. (3) The chain clustering or agglomeration of nanoparticles strengthens the local heat transfer by forming a low thermal resistance zone. The nanolayer is a developing layer formed by liquid molecules wrapped around nanoparticles in an intermediate state between fluid and solid, which is assumed to be a thermal connector between the base fluid and the nanoparticles on account of the ordered arrangement of molecules in this part. It is worth noting that unstable nanofluids can cause a decrease in thermal conductivity mainly due to the clustering of large



particles [25, 31 , 32].

Table 3 Summary of previous works on thermal properties of nanofluids used in solar spectrum splitters

Researcher, Year	Nanomaterial	Base fluid	Concentration	Fluid Temperature (°C)	Thermal conductivity
Yavari et al., 2019 [24]	Fe <sub>3</sub> O <sub>4</sub> / MWCNTs	Water	0.1wt%	-	Increased by 52% (H = 0.14T)
Rodriguez-Laguna et al., 2019 [32]	Graphene	DMAc/NM P/DMP	0.18wt%	20-21	Increased by 48%
Das et al., 2019 [33]	Graphene	Water	0.1wt%	45	Increased by 29%
Askari et al., 2019 [34]	MWCNTs	Kerosene	0.5wt%	60	Increased by 28%
Barai et al., 2019 [25]	Reduced graphene oxide-Fe <sub>3</sub> O <sub>4</sub> (rGO-Fe <sub>3</sub> O <sub>4</sub> )	Water	0.01, 0.05, 0.07, 0.1 and 0.2 vol.%	40	Increased by 41.35%, 57.23%, 66.76%, 77.72% and 83.44%, respectively.
Yang et al., 2019 [35]	Graphene	Water	0-1.5wt%	20-60	Increased by 48.1%
Vishnuprasad et al., 2019 [36]	Graphene	Water	0.2 vol.%	28	Increased by 57% (PH=7)
Maheshwary et al., 2020 [26]	CuO, MgO, TiO <sub>2</sub> , ZrO <sub>2</sub> and Al <sub>2</sub> O <sub>3</sub>	Water	2.5wt%	26.85-86.85	3.13 times the base fluid (cubic shaped Al <sub>2</sub> O <sub>3</sub> )
Xian et al., 2020 [27]	GnPs, TiO <sub>2</sub>	Water and EG	0.1wt%	60	Increased by 23.74%
Oraon et al., 2021 [28]	Sm-Co	Silicone oil	15wt%	-	Increased by 373% (H = 0.5T)
Pourrajab et al., 2021 [29]	Ag / MWCNTs	Water	0.04 vol% and 0.16 vol%	20-50	Increased by 47.3%
Cui et al., 2022 [37]	TiO <sub>2</sub>	Water	0.5-4.0 vol%	20-60	Increased by 19%
Liao et al., 2022 [38]	Cu	Ar	1.0-4.0 vol%	-	Increased by 92%
Bioucas et al., 2022 [39]	SiO <sub>2</sub> / ZrO <sub>2</sub>	Water and glycerol	0.03-0.10 vol%	19.85-79.85	Increased by 20%
Mukherjee et al., 2022 [40]	SiO <sub>2</sub>	Water	0.5 and 1 wt%	25–60	Increased by 19%
Chen et al., 2023 [41]	Cu	Ar	2.79 vol%	85K	Increased by 11.68%

### 3.3 Optical properties

Nanofluids as spectral splitting liquid display unique optical properties. Incident sunlight entering the nanofluid is absorbed, transmitted and scattered respectively as presented in Fig. 2; the optical properties of nanofluids depend on nature and combination parameters of base fluid and nanoparticles. Absorption is an essential parameter to assess the ability of fluid in capturing spectrum. In applications such as solar collectors, solar heating systems, and solar hot water systems, the absorption of incident sunlight has to occur and capture as much energy as possible. Transmission means that the sunlight passes through the medium without absorption and reflection. For PV cells, they need to transmit as much of their matching spectrum as possible to generate electricity, which otherwise will make PV cell excessively hot and ineffective. Likewise, the difference between nanoparticles and base fluid will also generate different spectral transmission ranges. Scattering is a phenomenon in which light is absorbed by irregularities or particles and released at somewhat different energies or wavelengths. It is significantly affected mainly by the concentration and size of nanoparticles. By adjusting size, morphology and concentration of nanoparticles as well as type, ratio and light range of base fluid can affect the optical properties.

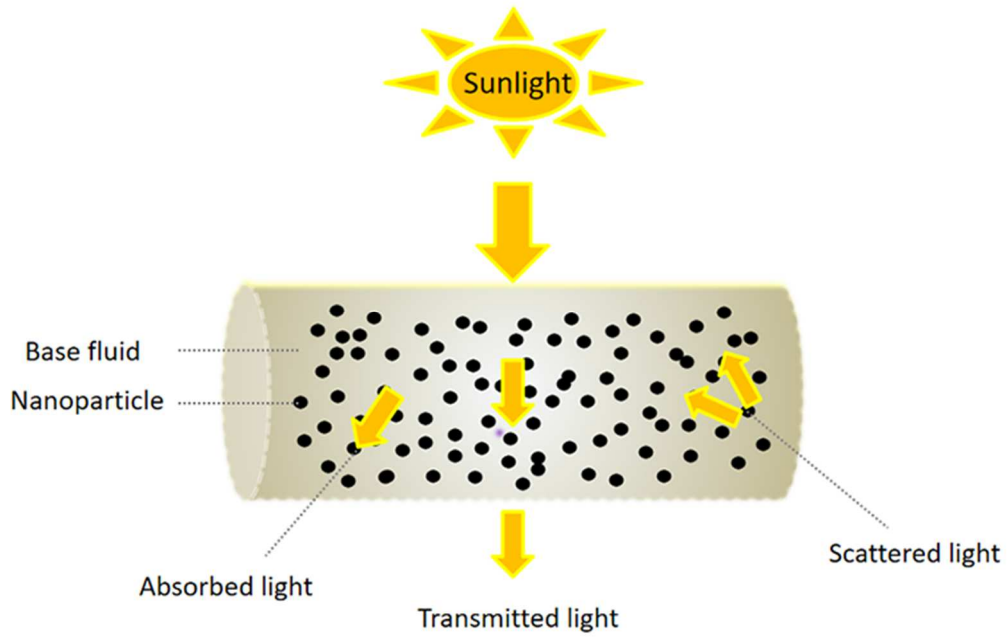


Fig. 2 Incident sunlight to nanofluid

From a theoretical point of view, the Rayleigh scattering model and the Mie scattering model are generally used to evaluate the optical properties of nanofluids depending on nanoparticle size through the parameter  $\alpha$  defined by equation (1). When  $\alpha \ll 1$ , the Rayleigh scattering model is applied; while  $\alpha \approx 1$ , the Mie scattering model is applied [42].

$$\alpha = \frac{\pi d_{np}}{\lambda} \quad (1)$$

where  $d_{np}$  is the nanoparticles diameter in nm and  $\lambda$  is the wavelength in nm.

The Rayleigh scattering theory is only valid isotropic spherical particles and nanoparticles volume concentration less than 0.6%. The optical factor of nanoparticles is given by the following three equations [43]:

$$Q_{e\lambda} = Q_{a\lambda} + Q_{s\lambda} \quad (2)$$

$$Q_{a\lambda} = 4\alpha \operatorname{Im} \left\{ \frac{m^2 - 1}{m^2 + 2} \left[ 1 + \frac{\alpha^2}{15} \left( \frac{m^2 - 1}{m^2 + 2} \right) \times \frac{m^4 + 27m^2 + 38}{2m^2 + 3} \right] \right\} \quad (3)$$

$$Q_{s\lambda} = \frac{8}{3} \alpha^4 \operatorname{Re} \left[ \left( \frac{m^2 - 1}{m^2 + 2} \right) \right]^2 \quad (4)$$

where  $Q_{e\lambda}$  is the extinction factor,  $Q_{a\lambda}$  is the absorption factor,  $Q_{s\lambda}$  is the scattering factor,  $m$  is the complex refractive index of the nanoparticles, and  $\operatorname{Im}$  and  $\operatorname{Re}$  are the imaginary and real parts of the complex refractive index, respectively. It is worth noting that (2) is suitable for base liquids with no absorption of incident light.

And in the Mie scattering theory, the optical factors are expressed by the following equations [44]:

$$Q_{e\lambda} = \frac{2}{\alpha^2} \sum_{n=1}^{\infty} (2n+1) \operatorname{Re}(a_n + b_n) \quad (5)$$

$$Q_{s\lambda} = \frac{2}{\alpha^2} \sum_{n=1}^{\infty} (2n+1) (|a_n|^2 + |b_n|^2) \quad (6)$$

where  $Q_{e\lambda}$  is the extinction factor and  $Q_{s\lambda}$  is the scattering factor. When the base liquids do not absorb the incident light, it also satisfies  $Q_{e\lambda} = Q_{a\lambda} + Q_{s\lambda}$ .

The spectral transmittance of the nanofluid can be found according to the Beer-Lambert-Bonguer law [45]:

$$\tau_{nl\lambda} = \frac{I_{\lambda}'}{I_{\lambda}} = e^{-e_{nl}\beta_{nl\lambda}} \quad (7)$$

where  $I_{\lambda}'$  and  $I_{\lambda}$  are the radiant illumination transmitted and received by the nanofluid in  $W/(m^2 \text{ nm})$ ,  $e_{nl}$  is the distance of light propagation in the nanofluid that is the liquid film thickness in  $nm$  and  $\beta_{nl\lambda}$  is the extinction coefficient of the nanofluid in  $nm^{-1}$ .

Simulation methods for optical properties of nanofluids usually include the Finite

Difference Time Domain (FDTD) method and the Monte Carlo Ray Tracing (Tracepro software) method. The FDTD method is an expressive time marching algorithm for solving Maxwell's curve equations on discrete space grids. Based on the model, transmission of sunlight in nanofluid can be simulated and spectral quantities of reflection as well as transmission can be calculated [46]. For a given volume concentration, mixing more small-sized particles with larger-sized particles can absorb more energy. This concept is illustrated by Duan et al. [46] who evaluated the optical properties of Ag@SiO<sub>2</sub>/water nanofluid under the excitation of plasma effect by FDTD simulation as presented in Fig. 3. The increase in size of core/shell nanoparticles broadens the spectrum of absorption, but nanoparticle absorption properties decrease with the increase of shell thickness. Red-shifting of absorption also occurs when the nanoparticle size increases. The nanofluid with randomly distributed particles in this study strongly absorbs wavelengths above 1500 nm. Liang et al. [47] investigated SiO<sub>2</sub> nanofluids using the Monte Carlo Ray Tracing method and Mie scattering theory. It is found that when the nanoparticle diameter is 5 nm, the scattering coefficient is small and the spectral transmittance is not varied with the increase of volume fraction, so the scattering effect of nanofluid can be ignored, while the nanoparticle diameter is larger than 15 nm, the spectral transmittance reduces significantly and the scattering coefficient is higher, hence the scattering needs to be considered. However, the effect of scattering on PT conversion efficiency of SiO<sub>2</sub> nanofluids is not significant. The increase in the scattering coefficient will reduce the PV conversion efficiency.

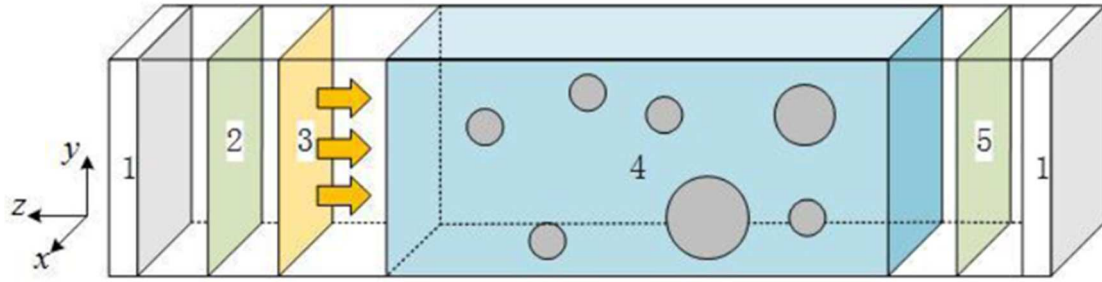
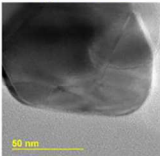
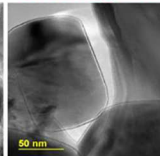
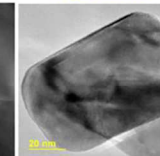
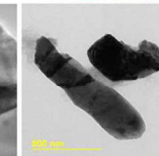


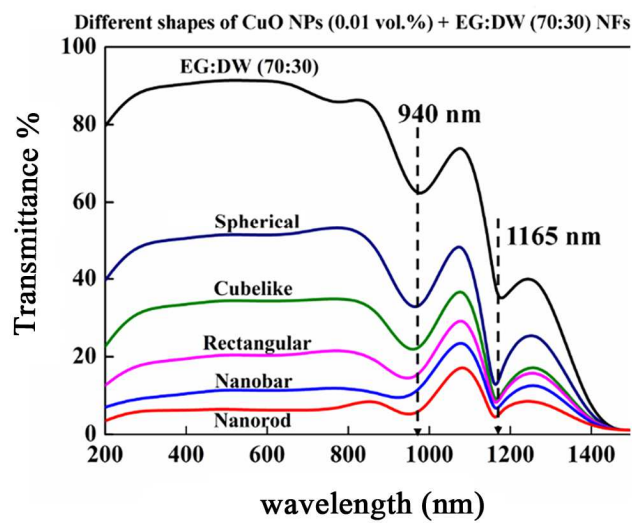
Fig. 3 Sketch of FDTD model: 1—PML layer, 2—reflection spectrum calculation plane, 3—incident plane, 4nanofluid, 5—transmission spectrum calculation plane [46]

Spectral transmittance testing is divided into traditional testing methods and dual optical range testing methods. The traditional test method produces interface errors during the measurement of empty cuvette and subsequent liquid, which makes beam transmission path change [10]. The dual-range test method uses the spectrophotometer to measure transmittance for two different thicknesses of liquid successively, and then eliminates the error caused by cuvette based on the Lambert-Bier law calculation. Shah et al. [48] examined the effect of CuO nanoparticle shape and size on optical properties of DW:EG based nanofluids as presented in Fig. 4. The spherical and nanorod shapes exhibited the highest and lowest transmission rates, respectively, under the same nanoparticle concentration. And the independent variables regarding the transmission function were found to be the shape and size of the nanoparticles by comparison tests on spherical, cube-shaped, rectangular, and nanorod shaped particles. The CuO nanofluid showed transmission drop within 940 and 1165 nm spectra. Hjerrild et al. [49] synthesized Ag@SiO<sub>2</sub> specifically in order to absorb most of the visible light and transmit it to corresponding cells. The addition of CNT to Ag@SiO<sub>2</sub>/water nanofluid reduced its transmission in the long wavelength spectrum and visible light fraction by

5-10%. Huaxu et al. [50] evaluated the effect of nanoparticle concentration transmittance in ZnO/ethylene glycol (EG) nanofluids. Since EG itself transmits visible light, the EG-based nanofluid exhibits no transmission in visible portion, which indicates that it is affected by nanoparticles. Experiments showed that the transmittance of nanofluids with ZnO nanoparticles concentrations of 1.2, 22.3, 44.6 and 89.2 ppm gradually increased in the UV shift to visible spectral region. Tong et al. [51] found that the maximum transmittance of Fe<sub>3</sub>O<sub>4</sub> nanofluid occurs near 850 nm spectrum. While in Fe<sub>3</sub>O<sub>4</sub> MWCNTs/water EG nanofluid the spectral transmittance decreases with the increase of MWCNT mass fraction and the maximum transmittance is merely 29%. Sajid et al. [52] investigated the effect of ultrasonication time and GA, CTAB and SDBS surfactants on the transmittance of Fe<sub>3</sub>O<sub>4</sub>/H<sub>2</sub>O nanofluid as spectral splitting liquid as presented in Fig. 5. The Fe<sub>3</sub>O<sub>4</sub> nanofluid without surfactant had a higher transmittance than that prepared with the surfactant for avoiding instability. And Fe<sub>3</sub>O<sub>4</sub> nanofluid with CTAB surfactant has better transmittance than that with GA or SDBS as surfactant. The transmittance of Fe<sub>3</sub>O<sub>4</sub> nanofluid with low concentration (0.0004%) showed a decreasing trend at 520 nm wavelength and then increased. The high concentration (0.004%) Fe<sub>3</sub>O<sub>4</sub> nanofluid absorbs strongly in visible spectrum, while there is slight transmission in near-infrared region.

<b>Reaction temp</b>	60°C/12h	80°C/12h	110°C/12h	160°C/12h	180°C/12h
<b>Crystallite size</b>	22.06 nm	23.09 nm	26.08 nm	26.92 nm	23.59 nm
<b>Dimensions</b>	Diameter 53.12 nm	Cube edge length 68.4 nm	Aspect Ratio 1.07	Aspect Ratio 1.57	Aspect Ratio 5.84
<b>NPs shapes</b>	<b>Spherical</b>	<b>Cubelike</b>	<b>Rectangular</b>	<b>Nanobar</b>	<b>Nanorod</b>
<b>TEM images</b>					

(a)



(b)

Fig. 4 The effect of shape and size on CuO nanofluid: (a) TEM images of CuO nanoparticles with different shapes and related information (b) Transmission spectra of different shapes of CuO nanoparticles nanofluid [48]



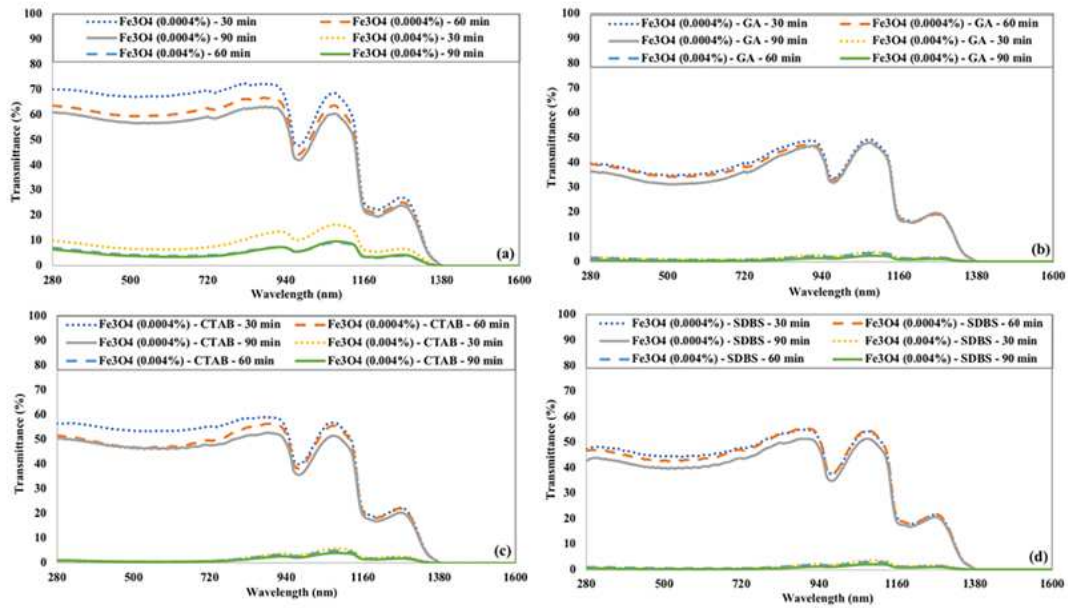


Fig. 5 The effect of ultrasonic time and (a) no surfactant (b) GA (c) CTAB (d) SDBS on the transmittance of Fe<sub>3</sub>O<sub>4</sub>/H<sub>2</sub>O nanofluid [52]

#### 4. Application of SBS in hybrid PV/T system

In this section, nanofluids produced with different nature of nanoparticles for SBS applications are presented in detail as gathered in Tables 4-6. The section is categorized into four classes of nanomaterials types respectively.

##### 4.1 Metal nanoparticles

The metal nanoparticles commonly used for splitting spectra mainly include Ag, Au and Cu, which are employed to absorb short-wave radiation as shown in Table 4. In order to achieve better response to silicon PV cells, it was proposed to disperse Ag nanoparticles in CoSO<sub>4</sub> solution to form nanofluid due to the strong absorption of CoSO<sub>4</sub> at short wavelengths [53]. Ag/CoSO<sub>4</sub> nanofluids with different concentrations were prepared and tested for their optical transmittance as well as efficiency as presented in Fig. 6. The results showed that Ag/CoSO<sub>4</sub> nanofluids exhibited superior

absorption performance than water-based nanofluids in the wavelength band less than 600 nm. A defined function of merit (FM) was introduced to evaluate the filtration performance of the system. It showed that the FM value of PV/T system based on Ag/CoSO<sub>4</sub> nanofluid is higher than that based on Ag@SiO<sub>2</sub>/H<sub>2</sub>O nanofluid and Ag/H<sub>2</sub>O nanofluid. Moreover, a maximum FM value is achieved with Ag nanoparticle mass fraction of 37 ppm [53]. Han et al. [54] dispersed Ag nanoparticles in CoSO<sub>4</sub> and PG base fluid to form nanofluid for matching Si and GaAs cells. The total efficiency of PV/T system with Ag/CoSO<sub>4</sub>-PG nanofluid filter is five times higher than that PV system alone. For the GaAs-based cells, the peak FM of PV/T system is 1.831 for nanoparticles mass fraction of 3 ppm and optical length of 43 mm. The specific value factors of using silicon CPV cells and GaAs cells in PV/T systems affect the FM value as presented in Fig. 7. Han et al. [10] presented plasmonic nanofluids containing Ag, Au and Cu nanoparticles for SBS. It was found that absorption summits appeared red-shifted when diameter of Ag nanoparticles and refractive index of base fluid were increased. The maximum FM value for Ag/PG-CoSO<sub>4</sub> nanofluid matched Si cells was 1.375 when nanoparticle diameter was 20 nm, concentration was 20 mg/L and optical length was 22 mm. Meanwhile the MF values of Cu nanofluid and Au nanofluid are also higher than Ag nanofluid. Given the high cost of Au and instability of Cu nanofluid, the MF of Ag nanofluid is greater when the nanoparticle size is small. These studies provide theoretical guidance for matching metal nanomaterials for Si and GaAs solar cells in the SBS applications of PV/T systems.

Abdelrazik et al. [55] investigated the dependence of transmittance for Ag/H<sub>2</sub>O

nanofluids on optical length and nanoparticles concentration. An experimental correlation between the all three was established. Fig. 8 presents the sketch for studied PV/T system with SBS. The higher transmittance is obtained in the 250 nm - 1400 nm band at short path lengths and low concentrations. The PV/T system with SBS application demonstrated better performance than the stand-alone PV system at low concentrations. Abdelrazik et al. [56] developed thermal, optical and electrical models to evaluate the performance of PV/T system with Ag/H<sub>2</sub>O nanofluid splitting. It generates both electrical and thermal energy with efficiencies of 8.4% and 66.7% at atmospheric temperature of 45°C and solar concentration of 5 KW/m<sup>2</sup> respectively. The electrical conversion efficiency of single PV cell is only 3.7% under the above conditions. However, the electrical performance is poor at atmospheric temperatures below 34.1°C in exception to the uniform solar concentration. The PV/T system with optical filtering exhibits superior performance chiefly at high atmospheric temperature and solar concentration conditions. The disadvantage of using nanofluids with precious metals (Au and Ag) is their high cost, and the solution is to perform complete economic analyses to explore whether the high price can be matched by the benefits.

A new PV/T collector design was proposed and tested with silicon cells using two types of filters based on Au and Ag nanoparticles nanofluids as presented in Fig. 9 [57]. Experimental and theoretical studies found that Ag nanofluid was able to achieve the highest PT efficiency, PV efficiency, and overall efficiency under the same particle diameter, volume fraction and channel thickness. The study by Saroha et al. [57] was a pioneering demonstration of nanofluid as viable multifunctional medium integrating

optical filtering and thermal transfer in PV/T solar systems. An et al. [58] applied nanofluid SBS system in solar distillation technology in which Ag-Au/H<sub>2</sub>O nanofluid was selected and generated electricity was passed through the components to produce water. It is observed that water production of the system with 26 ppm Au and Ag nanoparticles increased by 79.9% and 69.4% respectively compared to conventional system. At the same time, the thermal efficiency was enhanced by 6.8% and 4.8% respectively. These enhanced efficiencies were mainly due to the absorption of sunlight by water promoted with Au and Ag nanoparticles.

Table 4 Summary of previous works on metal nanoparticles nanofluids in SBS applications

Nanomaterial	Nanomaterial dimension (nm)	Base fluid	Concentration	Optical path	PV cell	Solar irradiance	PV efficiency (%)	PT efficiency (%)	Overall efficiency (%)
Ag [53]	29.9-65.0 nm	CoSO <sub>4</sub>	84.7, 31.8 and 5.3 ppm	10 mm	Si	1 KW/m <sup>2</sup>	5.27, 7.65, and 9.39%	46.73, 40.35, and 35.61%	52, 48 and 45%
Ag [54]	40-50 nm	CoSO <sub>4</sub> /PG	5.3, 15.9, 31.8, 63.5 and 84.7 ppm	30-50 mm	Si and GaAs	1 KW/m <sup>2</sup>	Si: 7.24, 6.98, 6.42, 5.18 and 4.56% GaAs: 9.31, 8.65, 7.32, 6.17 and 5.48%	61.14, 68.03, 73.40, 73.60 and 79.40%	Si: 68.38, 75.01, 79.82, 78.78 and 83.96% GaAs: 70.45, 76.68, 80.72, 79.77 and 84.88%
Ag, Au and Cu [10]	20-80 nm	water, water/CoSO <sub>4</sub> , PG and PG/CoSO <sub>4</sub>	1mg /L - 80mg /L	1mm - 60mm	Si and GaAs	1-30 KW/m <sup>2</sup>	Optimal is 7%	Optimal is 47.39%	Optimal is 54.39%
Ag [55]	18 nm	Water	0.0005, 0.001, 0.005, 0.01 and 0.05 wt %	2 mm, 5 mm, and 10 mm	-	992 W/m <sup>2</sup>	Optimal is 12.7%	-	-
Ag [56]	5-50 nm	Water	0.0005, 0.001, 0.005, 0.01 and 0.05 wt%	2-20 mm	-	5 KW/m <sup>2</sup>	Optimal is 8.4%	Optimal is 66.7%	Optimal is 75.1%
Ag and Au [57]	5, 10nm	Water	0.00019 vol% and 0.00025 vol%, 0.0193 vol% and 0.0093 vol%	6,7 and 10 mm	Si	1 KW/m <sup>2</sup>	Optimal is 9.6 %	Optimal is 68 %	Optimal is 77.6 %

Nanomaterial	Nanomaterial dimension (nm)	Base fluid	Concentration	Optical path	PV cell	Solar irradiance	PV efficiency (%)	PT efficiency (%)	Overall efficiency (%)
Ag and Au [58]	16-38 nm	Water	26 ppm	-	Si	Practical	Optimal is 3.6 % and 4.3%	Increase by 4.8% and 6.8%	Increase by 69.4% and 79.9%

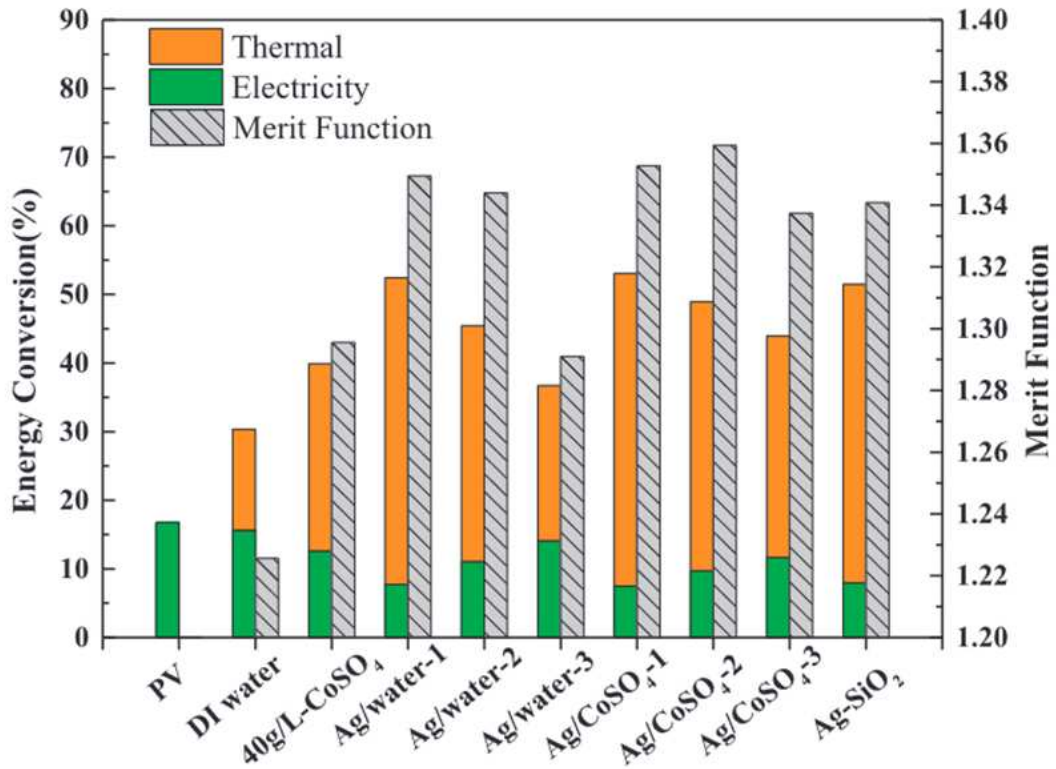


Fig. 6 PV and PT conversion efficiency as well as Function of Merit for each fluid

[53]

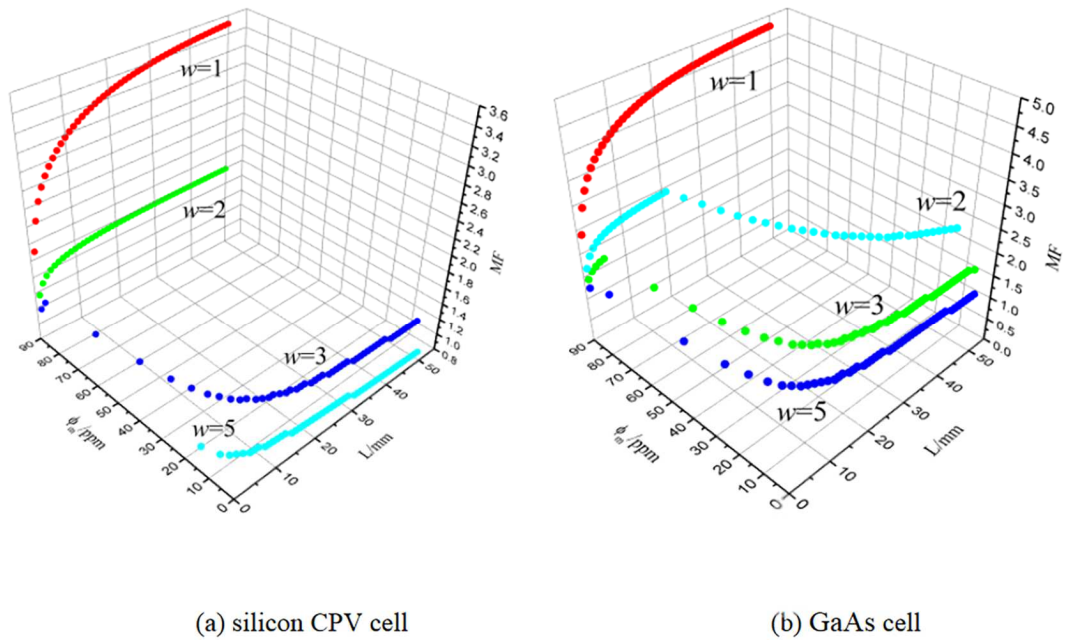


Fig. 7 Effect of value factors on FM values for PV/T systems using silicon CPV cells

(a) and GaAs cells (b) respectively [54]

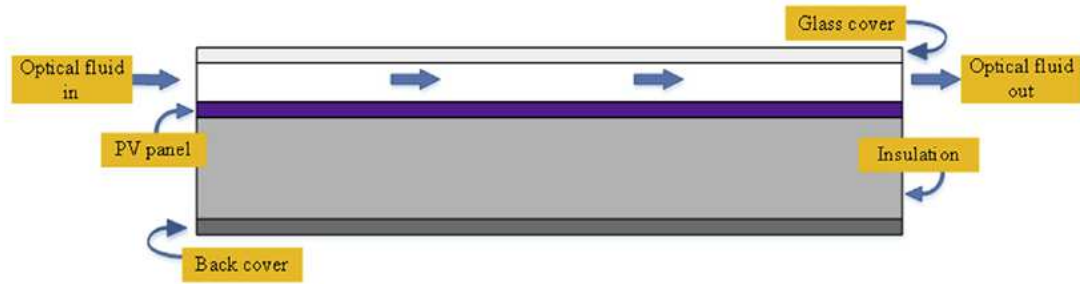


Fig. 8 Sketch of the SBS PV/T system designed by Abdelrazik et al. [55]

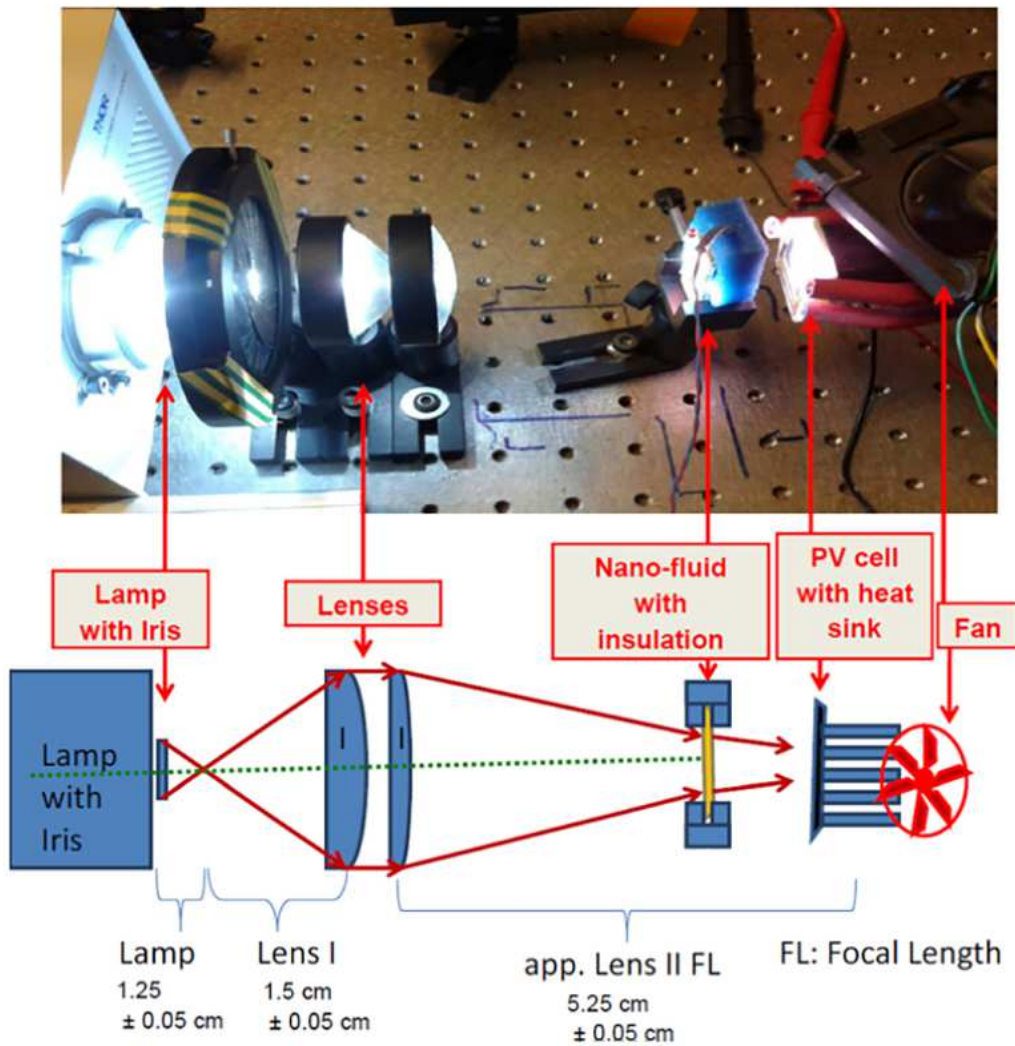


Fig. 9 Establishment of the indoor SBS PV/T system developed in [57]

#### 4.2 Metal oxide nanoparticles

Several types of metal oxide nanoparticles are used for splitting spectra as summarized in Table 5, and most researchers selected substances based on a



combination of optical properties, magnetic properties, and cost. Jin et al. [11] first proposed a novel magnetic electrolyte nanofluid (ENF) suitable for PV/T system splitting. ENF can be considered as liquid optical filter that allows intelligent regulation and control by an external magnetic field due to its magnetic properties. Two nanofluids were obtained by dispersing optimized amounts of  $\text{Fe}_3\text{O}_4$  nanoparticles in 50% water/50% EG solution containing methylene blue (MB) or copper sulfate (CS). The optical absorption of Si and InGaP PV cells were satisfied, respectively. In addition, the filtering performance of this ENF is evaluated based on theoretical model. It is shown that both ENFs have higher FM values than the water-based core@shell nanoparticle nanofluid filter and their optical path length is less. Abd El-Samie et al. [59] combined different nanoparticles (Ag,  $\text{Fe}_3\text{O}_4$  and  $\text{SiO}_2$ ) and different base fluids (water, therminol VP-1 and PG) to obtain nanofluids. The simulations revealed that  $\text{Fe}_3\text{O}_4$  nanoparticles with different base fluids can achieve the highest thermal performance. Among them,  $\text{Fe}_3\text{O}_4/\text{H}_2\text{O}$  showed the best absorption capacity and significantly improved thermal efficiency at particle concentration of 120 ppm. The energy output achieved in such system is 179%-240% higher than that in PV system alone.

Zhu et al. [60] experimentally studied optical properties of ZnO/water nanofluid in spectral range of 200 nm - 2000 nm and pointed out its possibilities for SBS applications. At nanoparticle mass fraction of 0.02 %, the transmittance of ZnO/water nanofluid gradually increases when wavelength is in the range of 200 nm - 800 nm. Therefore it is suitable for applications where visible light is highly transmissive. In addition, the Arabic gum dispersant reduces transmittance of base fluid by less than 5%

in wavelength range of 300 nm - 900 nm. Liang et al. [61] explored the possibility of ZnO nanoparticles for SBS applications from perspective of optical properties in consideration of their low-cost and good thermal conductivity. The ZnO/H<sub>2</sub>O and ZnO/EG nanofluids were tested for stability and model validation as well as evaluated for transmittance. The effective spectral transmittance of ZnO/H<sub>2</sub>O nanofluids was increased by 21.54% and 8.74% compared to nanofluids containing polypyrrole/H<sub>2</sub>O and Cu<sub>9</sub>S<sub>5</sub>/H<sub>2</sub>O respectively, which is closely related to its low absorption index. The spectral transmittance of ZnO/EG nanofluid in the UV-Vis band increases with decreasing nanoparticle size and decreases with increasing nanoparticle concentration. It also increased with the increase of optical length in the full studied wavelength band. Stability tests were also performed on ZnO/water and ZnO/EG nanofluids under high temperature (80°C) and UV illumination conditions as presented in Fig. 10. The results showed that the ZnO/EG nanofluid has better stability than the ZnO/water nanofluid. Liang et al. [50] also tested the feasibility of low-cost ZnO/EG nanofluid and built two-axis solar tracking-based nanofluid SBS hybrid PV/T system as presented in Fig. 11. The test results showed that solar energy conversion efficiency correlation index (SECE) based on ZnO/EG nanofluid was 21.8% and 5% superior than polypyrrole/water nanofluid and Ag@SiO<sub>2</sub>/water nanofluid respectively. The power generation efficiency of the PV cell was reduced from 16.33% to 14.49% when using the ZnO/EG nanofluid splitting, which is attributed to some incident light being absorbed by nanofluid and converted to thermal energy. These PT outputs compensate for the loss in cell efficiency and raise total system conversion efficiency. Moreover, the price of ZnO nanoparticles

is 0.08% of the price of Ag nanoparticles [50]. All of these data provide statistical guidance for ZnO nanofluid in SBS applications for PV/T systems.

Liang et al. [47] investigated the impact of SiO<sub>2</sub> nanofluid volume fraction and particle size on optical properties and solar energy conversion efficiency by Mie scattering theory combined with Monte Carlo ray tracing method. It was evidenced that the transmittance was not changed with the increase of volume fraction at nanoparticle size of 5 nm. The transmittance changes greatly when nanoparticle diameter is larger than 15 nm, so scattering should be considered at this stage. As the volume fraction and particle size of SiO<sub>2</sub> nanofluid increase, there is a slight growth in the energy absorbed by PT part. Therefore, the scattering of SiO<sub>2</sub> nanofluid has small effect on PT conversion, but the increase of scattering coefficient reduces PV efficiency and consequently the total conversion efficiency. Liu et al. [62] used PV/T systems with dual-channel nanofluid above and below PV modules as well as researched absorption performance of carbon, CuO, Al<sub>2</sub>O<sub>3</sub>, SiO<sub>2</sub>, and graphite nanofluids at 1% volume fraction. The SiO<sub>2</sub>/deionized water nanofluid had the greatest absorption performance with total output power of 2.609 W, which is followed by the carbon, graphite, Al<sub>2</sub>O<sub>3</sub> and CuO nanofluid systems respectively. However, Abd El-Samie et al. [59] found thermal efficiencies of the system using SiO<sub>2</sub> nanoparticles strongly changed with increasing nanoparticles concentration within volume fraction of 0 - 200 ppm tested in simulation.

Liu et al. [62] found CuO nanofluids exhibit high transmission (60%-70%) in the NIR region but low transmission in other regions. Therefore, little light reaches PV

module making the power output unsatisfactory. Similarly, Sajid et al. [52] discovered CuO nanofluids have extremely weak transmittance in the visible region and high transmittance in 700 - 1100 nm spectral region. Thus, CuO nanofluid is expected to be an ideal candidate for SBS in PV/T systems, and it is only necessary to improve the PV performance by tuning this fluid parameter so that the incident light in the response band of the matched cell is highly transmitted to reach the PV cell.

Ju et al. [63] presented a novel 2D:3D numerical simulation method for collectors using nanofluid splitting and evaluated the performance of SBS modules. The full coupling method (FCM) used considers solar inhomogeneity and direction of beam reflected to receiver as well as variation of optical properties of material used over solar irradiance thus increasing the authenticity. In addition, it was observed that the absorbance of thermalbands using Indium Tin Oxide (ITO)/Therminol VP1 oil nanofluid increased by 62.5% compared to base fluid. Meanwhile, the temperature of cell and transmitted irradiance declined significantly. As presented in Fig. 12, the PV cell surface temperature distribution and illumination are similar using base fluid filter and nanofluid filter, but the latter has significantly lower PV cell temperatures and improved temperature uniformity in the x-direction. This is particularly beneficial for the long-term efficient operation of PV cell and even the overall system.

Table 5 Summary of previous works on metal oxide nanoparticles-based nanofluids in SBS applications

Nanomaterial	Nanomaterial dimension (nm)	Base fluid	Concentration	Optical path	PV cell	Solar irradiance	PV efficiency (%)	PT efficiency (%)	Overall efficiency (%)
ZnO [50]	-	EG	11.2, 22.3, 44.6, and 89.2 ppm	5 mm	Si	816, 747, 718 and 645 W/m <sup>2</sup>	14.49, 14.14, 13.55 and 13.1%	7.4, 8.17, 9.19 and 10.97%	21.89, 22.31, 22.74 and 24.07%
SiO <sub>2</sub> [47]	5nm, 15nm, and 30nm	Water	0.5 vol%, 1 vol%, and 2 vol%	10 mm	Si	1 KW/m <sup>2</sup>	22.5%-25%	3.1%-3.3%	25.6%-28.3%
Fe <sub>3</sub> O <sub>4</sub> [11]	15 nm	Water/EG	-	10 mm	Si and InGaP	1 KW/m <sup>2</sup>	-	-	-
Ag, Fe <sub>3</sub> O <sub>4</sub> and SiO <sub>2</sub> [59]	2 nm	Water, therminol VP-1 and PG	120 ppm	2 mm	Si	0.4-1.4 KW/m <sup>2</sup>	14.7 %	47.2 %	61.9%
ZnO [60]	10 nm	Water	0.02 %	10 mm	Si	-	-	-	-
ZnO [61]	231 nm	Water	22.3 ppm	5-30 mm	-	1 KW/m <sup>2</sup>	-	-	-
Carbon, CuO, Al <sub>2</sub> O <sub>3</sub> , SiO <sub>2</sub> , and graphite [62]	-	Deionized water	1 vol%	3 mm	-	-	0.23%, 0.13%, 3.50%, 4.40% and 0.03%	69.57%, 41.37%, 41.37%, 82.57% and 60.57%	69.80%, 41.50%, 44.87%, 86.97% and 60.60%
CuO, Fe <sub>3</sub> O <sub>4</sub> [52]	< 50 nm and 50-100 nm	Water	0.004 vol% and 0.0004 vol%	10 mm	-	-	-	-	-
ITO [63]	-	Therminol VP1 oil	400 ppm	2 mm	Si	4 KW/m <sup>2</sup>	12.51%	48.10%	60.61%

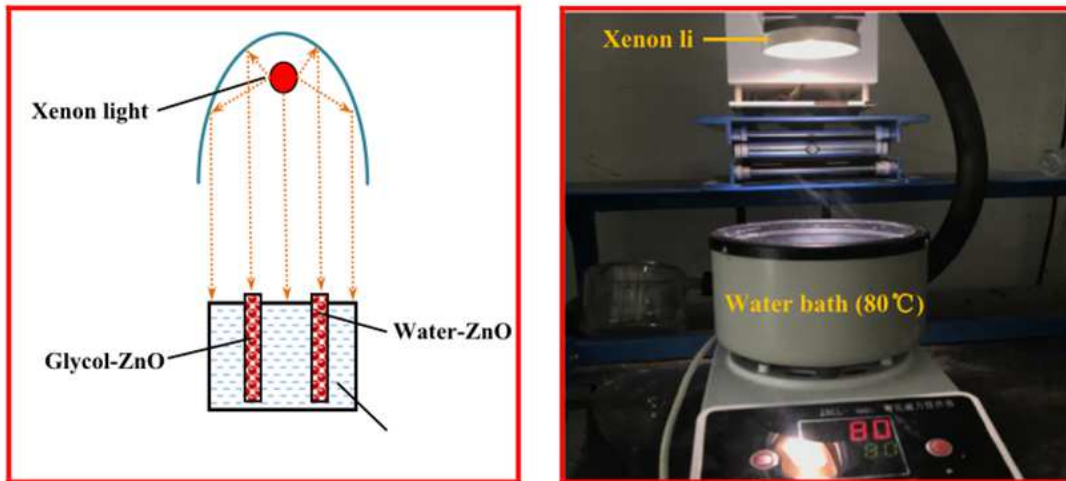


Fig. 10 Scheme and figure of stability test rig [61]

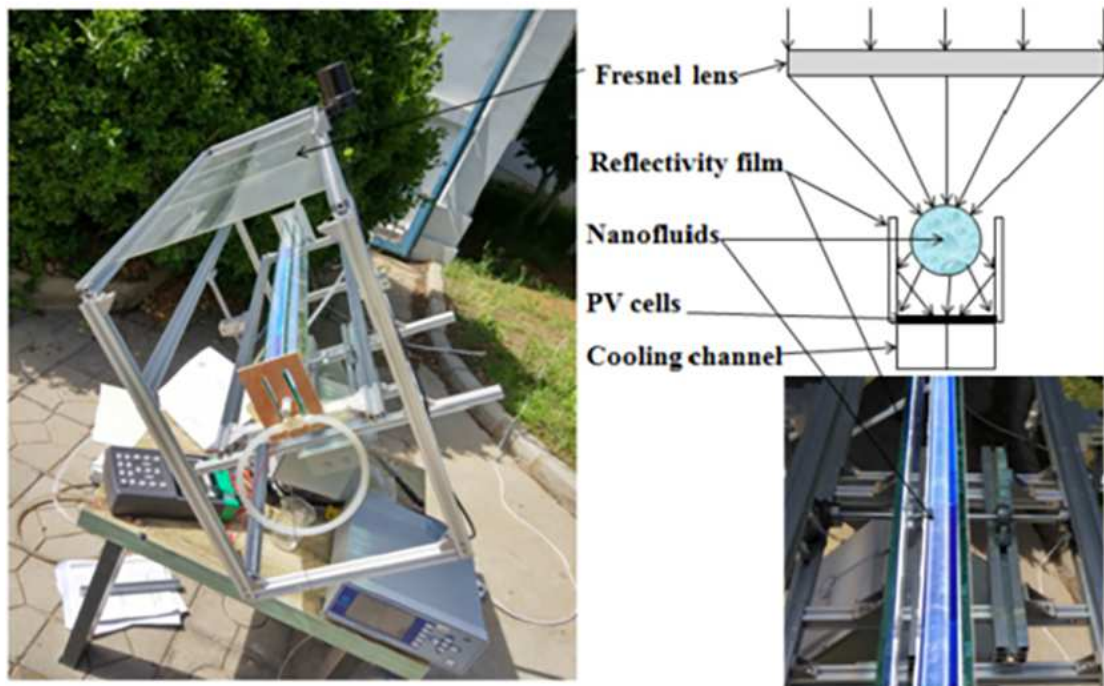


Fig. 11 The photograph of ZnO/EG nanofluids based SBS hybrid PV/T system [50]

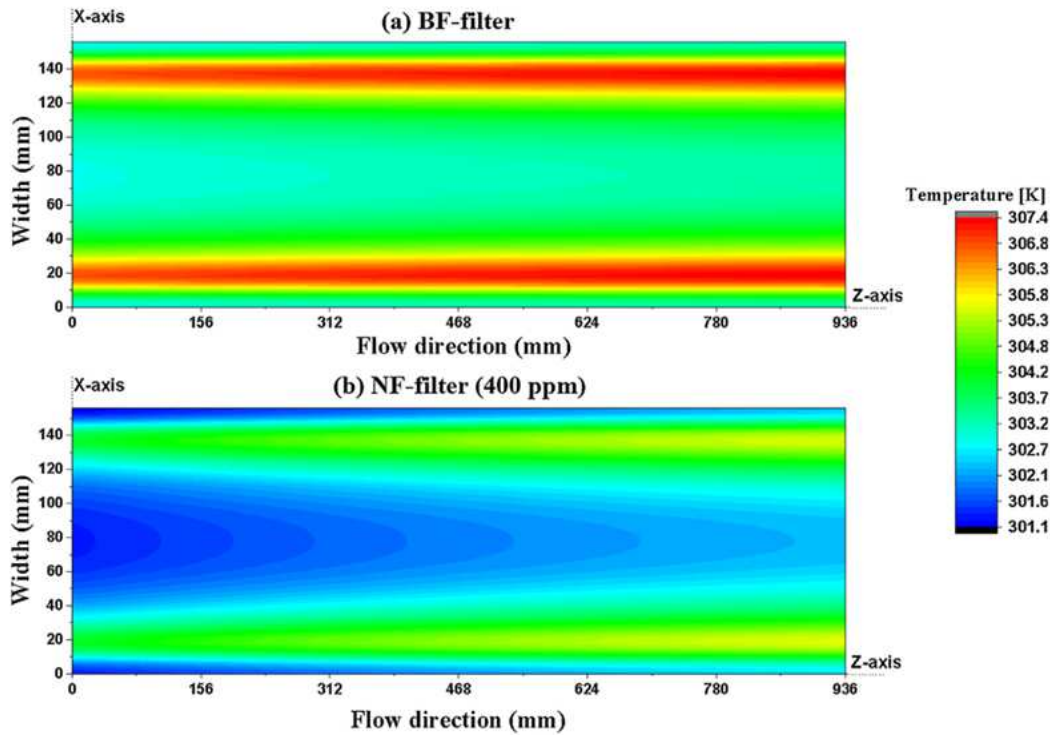


Fig. 12 Comparative temperature distribution of PV cell in SBS PV/T system using a) BF-filter and b) NF-filter (view of upper surface of PV cell) [63]

#### 4.3 Carbon based nanomaterials

Carbon-based nanomaterials are suitable for studies that focus on PT output or strengthen absorption without being the primary splitting material. Hjerrild et al. [49] pointed out that low concentration CNT solutions can be used to enhance absorption especially in UV part of the spectrum. Sajid et al. [52] examined the effects of ultrasonication time and surfactant on stability and optical properties of several nanofluids in SBS applications. Among them, CNTs/water nanofluid was the most stable at concentration of 0.004%, which showed average absorbance 67.6% and 74.6% higher than CuO and Fe<sub>3</sub>O<sub>4</sub> nanofluids, respectively. Due to the limited absorption range of CNT broadening, SBS with nanofluids containing only one type of CNT nanoparticles is rarely studied. The literature on carbon-based nanomaterials in the field

of SBS is indeed scarce but exists. In addition, carbon-based nanomaterials are generally mixed with another material and rarely perform SBS alone. It is frequently used to enhance properties by mixing with other materials under specific conditions.

An SBS PV/T system based on polypyrrole nanofluid was developed by An et al. [64] in order to accomplish high temperature thermal output. As presented in Fig. 13, sunlight passes through fresnel lens to nanofluid flowing in quartz tube, which acts as optical filtering and heat transfer fluid (HTF). It converts the absorbed infrared spectrum into thermal and the remaining sunlight is transmitted to reach customized polycrystalline silicon cell set. This SBS system with polypyrrole nanofluid has overall efficiency of up to 25.2%, which is 13.3% improvement over the system without filter. Further, the experimental results show that nanofluid temperature and efficiency of PV cell rised but decrease in PT conversion when nanoparticle concentration increases. Liang et al. [50] found that solar energy conversion efficiency correlation coefficient of SBS system based on polypyrrole/water nanofluid was 0.63, which was 0.218 lower than ZnO/EG nanofluid when particle concentrations were 12.5 ppm. Moreover, the cost of polypyrrole nanofluid is high and not available for mass production. Although polypyrrole can be used in SBS field but it is obviously not the most appropriate material. Most of the carbon-based nanomaterials studied currently are suitable for direct absorption collectors, and their use in SBS directly reduces the PV efficiency.



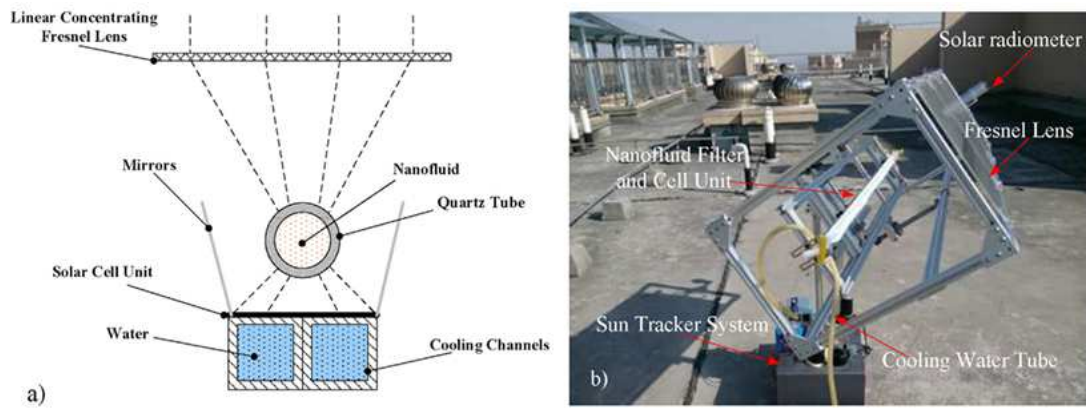


Fig. 13 The photograph of polypyrrole nanofluid based SBS hybrid PV/T system [64]

#### 4.4 Complexes of metals and metal oxides: Core@shell nanomaterials

Core@shell nanomaterials consist of a material completely encapsulated in another particle. This composite structure superimposes the optical properties of both substances and simultaneously protects the core (usually noble metal) to maintain shape as well as to increase dispersion by making it less likely to aggregate. Information about the use of core@shell nanofluids in SBS is shown in Table 6. For PV/T conversion in cold regions, an Ag@TiO<sub>2</sub>/EG/water nanofluid splitter is proposed to be feasible and can operate at about - 45 °C, which is much lower than using water alone as base fluid (freezes at about 0 °C) [65]. The shape and size distribution of core shell can be clearly seen in Fig. 14. The PT efficiency rises with increasing nanoparticle concentration but the PV efficiency follows an opposite trend as presented in Fig. 15. And the PV efficiency is only 5.6% when nanoparticle concentration is 200 ppm, which is much less than the efficiency of PV cell itself (19%). This is due to the fact that nanofluid absorbs part of light energy before PV cell converts energy, obtaining thermal energy which makes the overall conversion efficiency much higher and offsets the loss of PV efficiency. In addition, keeping the optical concentration at low level allows cells to

remain cool in absence of thermal sink [65].

Ag@SiO<sub>2</sub> is the most commonly used of all core-shell materials in SBS. Since the Ag nanodiscs can intensely absorb short waves and the SiO<sub>2</sub> shell not only keeps shape but also increases dispersion stability of silver core making it less likely to agglomerate. The adjustment of SiO<sub>2</sub> shell thickness can also modify the optical properties of nanofluid. Crisostomo et al. [66] designed and built a real SBS hybrid PV/T system operating outdoors by suspending Ag@SiO<sub>2</sub> nanoparticles in water as beam splitter for silicon photovoltaic cells. The nanofluid was placed in translucent tube to both filter the incident light and act as HTF. Three different Ag solutions were compared according to spectral response curve of silicon cell to finally receive transmitted sunlight from 713nm - 1100nm. The tests showed that this system improved the weighted energy output by more than 12% over the stand-alone PV system under same illumination conditions, which can be extended to cogeneration applications. Huang et al. [67] prepared Ag@SiO<sub>2</sub>/CoSO<sub>4</sub>-PG nanofluid with tunable silicon shell thickness as beam splitter with optical properties. It was found to be highly transmissive in range of 615 nm - 970 nm and highly compatible with silicon concentrator solar cells as well as calculated filtration efficiency of 39.3%. The total efficiency of the system with 25.4 mg/L Ag@SiO<sub>2</sub>/CoSO<sub>4</sub>-PG nanofluid was increased by 63.3% and economic value was increased by 67.8% at relative value factor (w) of 3. Then Huang et al. explored stability of Ag@SiO<sub>2</sub> nanofluids and its optimization for PV/T receivers in [68]. They found that Ag@SiO<sub>2</sub>/PG nanofluids can still maintain stable optical properties after 60 days of preservation in high temperature and radiation environment. Furthermore the

optimization method for selecting the best particle concentration and optical distance was established by Mie scattering theory and Lambert Beer's law. The filtering efficiency of GaAs and Si solar cells exceeded 35% and 43%, respectively. Meanwhile, Zhao et al. [69] found that Ag@SiO<sub>2</sub>/PG nanofluid exhibited excellent thermal stability without agglomeration when heated at 120°C. The specific efficiency and MF variation with optical path length as well as nanoparticle concentration are also presented in Fig. 16.

To achieve more perfect spectral match in SBS PV/T system, several studies have employed spectrally tailorable nanofluids mixed with multiple nanoparticles as the spectral splitting liquid. Hjerrild et al. [49] proposed that Ag@SiO<sub>2</sub> nanodiscs and CNTs were suspended in water to form nanofluid placed between light source and silicon cell. The core-shell particles are used to absorb most of visible light and low concentration CNT solution to enhance absorption especially in UV. Their study showed that Ag@SiO<sub>2</sub> nanoparticles suspended in CNT base fluid produced higher FM than water-based Ag@SiO<sub>2</sub> nanoparticles despite the fact that CNTs do not have selective absorption properties. Furthermore, Hjerrild et al. [12] tested SBS nanofluid for C-Si, GaAs and Ge solar cells. The nanofluids contained Ag@SiO<sub>2</sub> nanoplates absorbing visible light and silica-coated gold & gold-copper nanorods absorbing infrared spectra. Different concentrations of nanoparticles were suspended in water or oil-based fluids according to the response wavelengths of three cells. The results indicated Ag@SiO<sub>2</sub>/water nanofluid with C-Si PV cells had the highest efficiency in their configuration which is a promising candidate for low cost and high efficiency SBS

technology.

Table 6 Summary of previous works on composite nanoparticles based nanofluids in SBS applications

Nanomaterial	Nanomaterial dimension (nm)	Base fluid	Concentration	Optical path	PV cell	Solar irradiance	PV efficiency (%)	PT efficiency (%)	Overall efficiency (%)
Ag@SiO <sub>2</sub> [46]	15 nm, 30 nm and 45 nm @ 5nm	Water	0.01vol%	-	-	-	-	-	-
Ag@SiO <sub>2</sub> /CNT [49]	17.5nm/1μm	Water	0.006wt%/0.067wt%, 0.003wt%/0.078% and 0.001wt%/0.083wt%	10 mm	Si	10 KW/m <sup>2</sup>	9%, 10%, and 11%	43%, 40% and 37%	52%, 50% and 48%
Ag@TiO <sub>2</sub> [65]	21.6 nm @ 2.0 nm	EG/water	0, 50, 100, and 200 ppm	14 mm	Si	1 KW/m <sup>2</sup>	~13%, 9%, 7% and 5%	~41.1%, 61.7%, 67.8% and 78.7%	54.1%, 70.7%, 74.8%, and 83.7%
Ag@SiO <sub>2</sub> [66]	50 nm	Water	0.025, 0.019, 0.013 and 0.06 wt%	12 mm	Si	892 W/m <sup>2</sup>	-	-	18.9%, 23.4%, 32.5% and 33.2%
Ag@SiO <sub>2</sub> [67]	33 nm @ 34 nm	CoSO <sub>4</sub> -PG	5.1 mg/L, 12.7 mg/L, 25.4 mg/L and 50.8 mg/L	10 mm	C-Si	1 KW/m <sup>2</sup>	9%, 8.8%, 8.1% and 7.6%	51.0%, 52.2%, 55.2% and 57.5%	60%, 61%, 63.3% and 65.1%
Ag@SiO <sub>2</sub> [68]	33 nm @ 30 nm	PG-DI and PG-CoSO <sub>4</sub>	30 mg/L, 50 mg/L, 23 mg/L and 9 mg/L	42 mm, 11 mm, 50 mm and 20 mm	GaAs and Si	1 KW/m <sup>2</sup>	-	-	Filtering efficiency: 43.78%, 39.02%, 35.55% and 26.62%

Nanomaterial	Nanomaterial dimension (nm)	Base fluid	Concentration	Optical path	PV cell	Solar irradiance	PV efficiency (%)	PT efficiency (%)	Overall efficiency (%)
Ag@SiO <sub>2</sub> [69]	-	PG	5.1, 12.7, 25.4, and 50.8 mg/L	2-50 mm	Si	1-30 KW/m <sup>2</sup>	Optimal is 17%	Optimal is 55%	Optimal is 72%
Ag@SiO <sub>2</sub> , Au/AuCu@SiO <sub>2</sub> [12]	-	Water/PG-1	38.7, 19.2 and 38.7 mg/L	10 mm	Ge, GaAs and C-Si	6000 ± 420 W/m <sup>2</sup>	Optimal is 15%	Optimal is 35%	Optimal is 40%

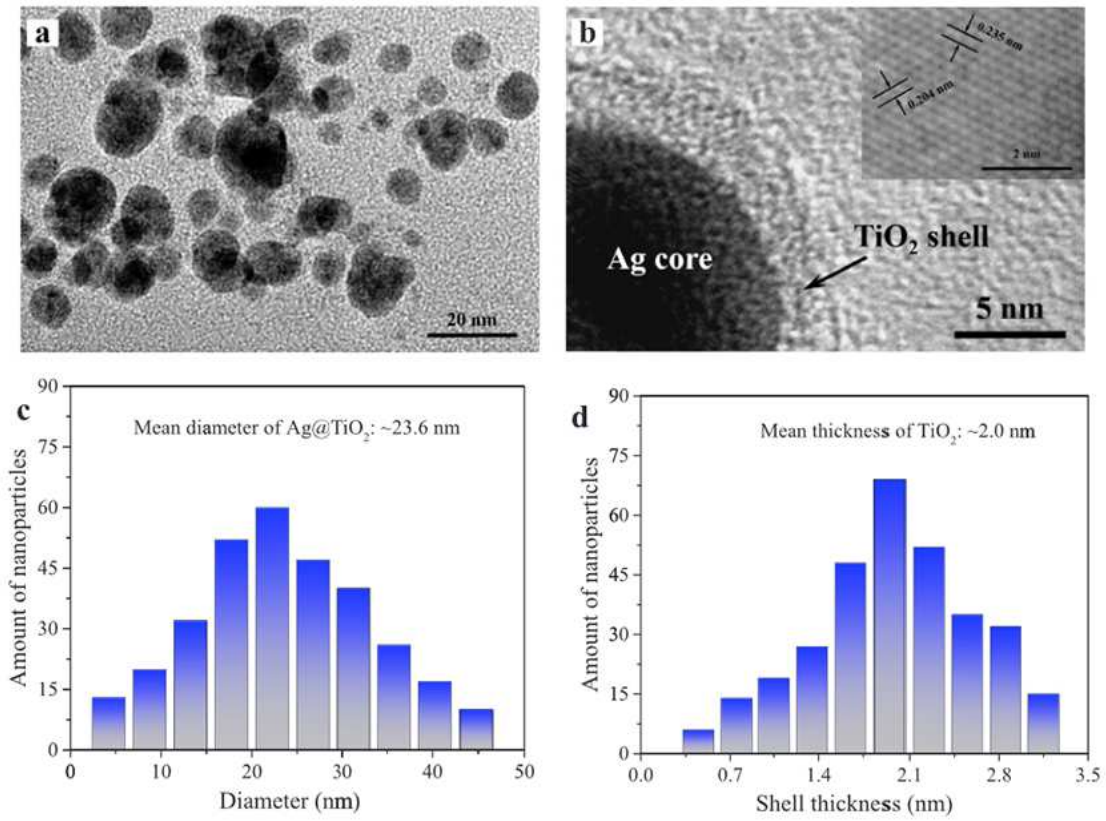


Fig. 14 The TEM image of Ag@TiO<sub>2</sub> nanoparticles [65]

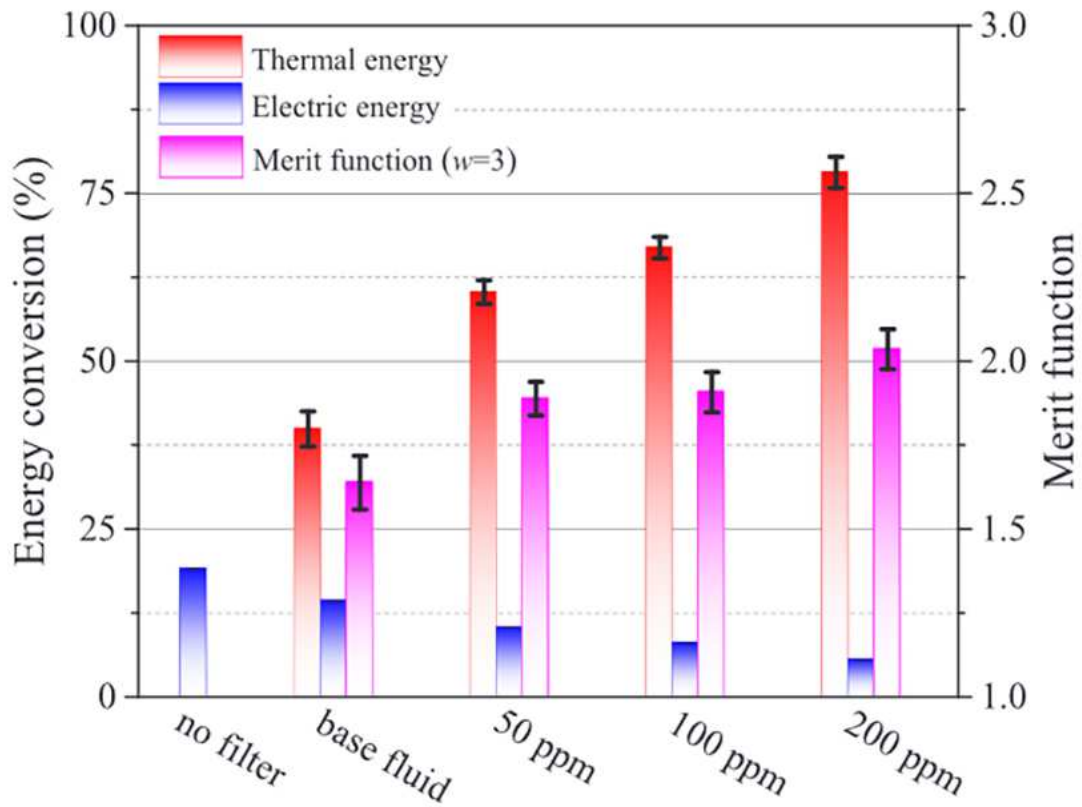


Fig. 15 Energy conversion efficiency and merit function for applying different

concentrations of Ag@TiO<sub>2</sub>/EG/water nanofluid splitting [65]

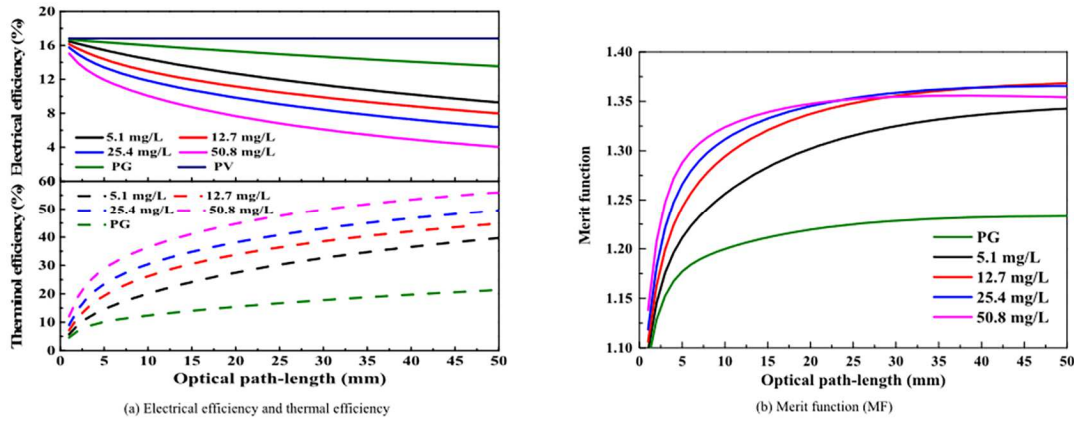


Fig. 16 The influence of nanoparticle concentration and optical path length on the thermal efficiency, electrical efficiency and MF of the PV/T system with

Ag@SiO<sub>2</sub>/PG splitting [69]

An analysis of the previous sections highlights the following conclusions. The magnetically optimized Fe<sub>3</sub>O<sub>4</sub>/H<sub>2</sub>O nanofluid is prospective for use as liquid optical filter for PV/T systems because it is an efficient and intelligent fluid that can be controlled by external magnetic field and has high stability and excellent thermal conductivity. Fe<sub>3</sub>O<sub>4</sub>/H<sub>2</sub>O nanofluid is the ideal choice for InGaP cells in the splitting spectrum. Ag@SiO<sub>2</sub> nanofluids are ideal for SBS since they absorb at wavelengths below 700 nm and above 1200 nm to better match Si cells in wide range of applications. In addition, the choice of two composites not only superimposes the optical properties but also the modification of Si - coated makes Ag nanoparticles less likely to aggregate and thus more stable in dispersion. The optimal liquid filter for GaAs cells is Ag nanofluid, where the FM value reaches 1.342 for Ag nanoparticle size of 20 nm, concentration of 1 mg/L, optical path length of 60 mm, and base fluid of PG. ZnO/EG nanofluid is the most cost-effective material in all SBS applications.



## 5. Cost analysis of NFs based SBS hybrid PV/T system

The cost of nanofluid as spectral splitting liquid is an important criterion in the selection of practical applications, which usually depends on the materials and dosage itself. The market price of ZnO nanoparticles of about \$0.285/g is the most economical among the available information, followed by Ag nanoparticles of \$35.7/g, polypyridine nanoparticles of \$167/g and Au nanoparticles of \$214/g in that order [61]. Dmour et al. [70] argued that what limits the development of Au and Ag nanoparticles in SBS is their high cost in addition to their weak UV absorption. Therefore, they proposed a nanofluid hybrid of antimony tin oxide nanoparticles and carbon quantum dots, which is not only inexpensive but also shows excellent stability and frequency division properties. Martínez-Merino et al. [71] used tungsten disulphide nanofluids to save the cost of selective coating of a parabolic trough collector, enabling a more cost-effective volumetric collector. Abdelgaied et al. [72] performed a complete economic analysis of the modified hemispherical solar evaporator (MHSS) using CuO/water nanofluid and paraffin as phase change material (PCM). The total distillate cost per liter of the MHSS containing paraffin, CuO/water nanofluid, and the blend of the two was 0.00905, 0.00719, and 0.00645, respectively. The combination of paraffin and 0.3 wt% of CuO/water nanofluid was used in the MHSS to reduce the cost of freshwater production over the conventional hemispherical solar evaporator by 75.0%, whereas the productivity was increased by 80.20%.

There are also nanofluids that are used instead of conventional fluids that do not directly reduce the cost, but save costs by improving the overall system performance

and increasing the benefits. Yan et al. [73] prepared hybrid nanofluids of white graphene and solar salts that have excellent thermal properties due to the large specific surface area of the white graphene and the ultra-high thermal conductivity. This hybrid used 12.82%, 29.8% and 76.79% increase in liquid phase specific heat capacity, solid phase specific heat capacity and solid phase thermal conductivity, respectively, over the pure solar salt. The increase in specific heat capacity and thermal conductivity significantly and indirectly reduces the cost. Farooq et al. [74] synthesized TiN nanoparticles by laser ablation. This resulted in an 80% increase in the thermal efficiency of TiN nanofluids in direct absorption solar collectors, and crucially, this technique offers considerable relative cost effectiveness. Gao et al. [75] first found that the incorporation of SiO<sub>2</sub> nanoparticles into molten salt nanofluids can inhibit the corrosion of stainless steel. The reason was the formation of silica corrosion layer structure on the surface of stainless steel. Then, Navarro et al. [76] explored the corrosive properties of SiO<sub>2</sub> nanoparticles of different concentrations on alloys in concentrated solar power plants. SiO<sub>2</sub> nanoparticles mixed in industrial grade solar salt were found to corrode stainless steel 304H the fastest. Suitability assessment showed that molten salt nanofluids for long term high temperature applications can be used with Inconel 600, 304H and 316L to reduce corrosion costs and increase service life.

Wciślik et al. [77] calculated the price of nanofluid preparation based on market prices according to the following formula, that depends on on the concentration of nanoparticles with specific sizes as gathered in Table 7. The calculation formula is given below:

$$C_{Nano} = \frac{c_u \rho V}{0.001} + C_{other}, \frac{EUR}{dm^3} \quad (8)$$

$$C_T = C_{Nano} + C_{Base}, \frac{EUR}{dm^3} \quad (9)$$

where  $C_{Nano}$  is the unit price of nanofluids,  $c_u$  is the unit cost of purchasing nanoparticles in EUR/g,  $\rho$  is the fluid density,  $V$  is the fluid volume,  $C_{other}$  is the extra costs,  $C_T$  is the total unit costs, and  $C_{Base}$  is the base fluid unit price.

Said et al. [78] added different weights of nanoparticles to silicone oil to enhance thermal conductivity and performed the system economic analysis. When adding 0.10 wt% Ti<sub>3</sub>C<sub>2</sub> nanoparticles reduces the system cost by 0.021 M\$ and the environmental benefits in terms of energy studies are 32.73 to 33.28 USD/year. The following is the economic feasibility assessment equation used:

$$V_{ST} = \frac{E_{SST}}{\rho_F \cdot C_F (T_{out} - T_{int})} \quad (10)$$

$E_{SST}$  denotes the thermal energy required to store and drive the system.

Seyyedi et al. [79] pointed out that increasing the concentration of nanoparticles certainly increases the heat transfer, but it is important to note that it also adds to the cost of production of nanofluids. Therefore the simple economic analysis was carried out to evaluate the thermal performance using the following equation:

$$C_T = C_{NP} + C_{BF} + C_{Other} \quad (11)$$

$$C_{NP} = cm \quad (12)$$

where  $C_T$  is the total unit cost of the nanofluid,  $C_{NP}$  is the cost of the nanoparticles in EUR,  $c$  is the unit price of the nanoparticles per gram,  $m$  is the mass, and  $C_{BF}$  and  $C_{Other}$  represent the unit price of the base fluid and other additional costs of

preparation, respectively.

Liang et al. [50] performed economic analysis using nanofluids comprising ZnO nanoparticles costing \$0.285/g and \$0.0004/g of EG. They used the net present value (NPV) to evaluate the investment of SBS hybrid PV/T system which was formulated as :

$$NPV = -C_0 + \sum_{i=1}^t \frac{C_i}{(1+r)^i} \quad (13)$$

Where  $C_0$  is the initial investment,  $C$  is the net cash flow,  $r$  is the discount rate and  $t$  is the period. The capital payback period of the SBS hybrid PV/T system based on ZnO/EG nanofluid was found to be 17 years in laboratory scale tests by NPV analysis. Yet its payback period would be significantly shorter if produced on large scale in practical applications. However, nanofluids have not yet achieved widespread real application in the field of SBS and there is not enough data to support assessed cost. Comprehensive economic analysis and cost reduction is needed for future SBS research optimization.

Table 7 Total unit cost for the preparation of different nanofluids [77]

Nanofluid	Nanoparticle size (nm)	Concentration (vol%)	Nanofluid total costs (of 1 dm <sup>3</sup> ,EUR)
TiO <sub>2</sub>	4-8	0.04	3.03
		0.07	5.26
		0.1	7.48
Al <sub>2</sub> O <sub>3</sub>	<50	0.04	1.4
		0.07	2.4
		0.1	3.4
SiO <sub>2</sub>	10-25	0.04	1.19
		0.07	2.02
		0.1	2.86
Ag	<100	0.04	223.47
		0.07	391.01
		0.1	558.54

## 6. Conclusions and future development

## 6.1 Conclusions

The nanofluid as spectral splitting device and HTF not only separates PV&PT units so that PV cells can serve efficiently at relatively low temperatures for a long time, but also avoids secondary heat exchange in applications, which is promising for the effective utilization for full spectrum of solar energy. The following conclusions can be drawn from the review of literature over the last decade:

- Systems where nanofluids are employed as splitting devices are far more efficient than other systems that utilize solid or liquid splitting, especially in terms of thermal output efficiency. Nanofluids can broaden absorption spectrum, which is needed to widen the non-visible portion, allowing the visible portion containing most of the energy to be converted to electrical energy by the cell.
- Nanofluid as splitting fluid needs highly well-dispersed stability to make itself less susceptible to changes in thermal and optical properties, and the process of maintaining stability is crucial to the total system performance.
- Nanofluids are uniquely qualified in terms of thermal performance. The higher thermal conductivity is also beneficial for SBS PV/T systems due to the increased heat transfer efficiency. At the same time, the properties of nanofluid and synthesis method directly affect thermal properties (thermal conductivity).
- The concentration, nanoparticle size, optical path length and base fluid of nanofluid can be dynamically adjusted according to the actual demand to better transmit the spectrum of responding PV cell part with high transmission and absorb the rest of spectrum with high absorption. It is worth noting that when the diameter of

nanoparticles is larger than 15 nm, variation of spectral transmission rate with increasing volume fraction is obvious and the effect of scattering needs to be considered. SiO<sub>2</sub> nanoparticles can be chosen when the volume fraction is too great because the scattering of this nanoparticle has less effect on the PV/T system.

- In contrast to the PT conversion efficiency, the PV conversion efficiency tends to show decreasing trend with the increase of nanoparticles. It is even lower than the efficiency of PV cell itself. This is because partial incident light is absorbed by nanofluid before reaching the cell to be converted to thermal energy output, which is sufficient to compensate for the decrease in electricity generation efficiency.
- The core@shell nanofluid composite of the two materials has not only overlapped optical properties and shape retention but also gained dispersion stability.
- Fe<sub>3</sub>O<sub>4</sub>/H<sub>2</sub>O nanofluid, Ag@SiO<sub>2</sub> nanofluid and Ag nanofluid are the optimum matching splitting nanofluids for InGaP cells, Si cells and GaAs cells, respectively.

## 6.2 Future development

However, although PV/T systems containing spectral filters obtain high theoretical efficiencies, the investment cost and maintenance are usually more expensive than PV cells and have not been developed for large-scale practical applications. For its feasibility, the increased efficiency should be able to offset this added cost. Therefore, future work of SBS utilization in PV/T solar systems needs to be succeeded by some theoretical studies and problem solving as follows:

- One of the key factors limiting the widespread use of nanofluids in SBS is their stability. The effectiveness of their properties decreases with time owing to the

instability. Particular attention should be paid to the effect of external operating conditions such as confinement, high temperatures and magnetic fields on the stability of nanofluids. Enabling nanofluids to maintain high stability while operating at temperatures higher than 200°C is a major challenge. It is necessary to obtain long-term stable nanofluids with good optical and thermal properties by perfecting the preparation technique. At the same time, most of the studies use one solar radiation intensity for experiments. Study in the effect of multiple solar radiation intensities and actual outdoor conditions on the system is a promising avenue to investigate.

- A dynamic system for cooling solar cells using spectral splitting is a well-designed way to improve the overall performance from multiple perspectives. However, this cooling technology has some problems for further development. (1) Most of the materials used for the spectral splitting vessel are glass or quartz, which are very fragile and do not meet the stress requirements in industry. Attempts were made to find a type of material that could solve the above problems and be manufactured on large scale at low cost. (2) The thermal resistance of the splitting container should be minimized to avoid unnecessary heat loss. (3) There is a lack of quantitative relationship between the thickness of the splitting layer and the efficiency of the cell as well as the absorbed heat. How to maximize the efficiency should be the focus of future design studies.
- There is a gap in the research of adjusting the spatial distribution of nanoparticles to control the selective absorption and transmission spectral range in order to

achieve effective matching of the full spectrum.  $\text{Fe}_3\text{O}_4$  nanoparticles are magnetic and intelligently tunable nanoparticles that can be preferentially selected for such research.  $\text{Fe}_3\text{O}_4$  coated Ag in core-shell structure nanomaterials can not only be induced by magnetic field but also increase the dispersion stability of the noble metal, which compounds the two absorption characteristic peaks offering the possibility of better matching the cell. However, there is the research gap of  $\text{Ag}@\text{Fe}_3\text{O}_4$  in SBS, which deserves in-depth experimental analysis.

- A more complete long-term economic analysis including up-front investment and post-maintenance is needed to ensure that the increased cost over a stand-alone PV system is counterbalanced by the efficiency it brings before the wider practical application of SBS. Also, attention should be paid to the actualized price of nanofluid and the additional expense of ensuring stability at high solar radiation.
- From the current literature review, it is evident that there is shortage of studies on optical characterization of some nanomaterials such as Cu, Cr, MgO,  $\text{NiFe}_2\text{O}_4$ , etc. There are also very few studies on ionic liquids in base fluids.

#### Acknowledgements

This study is financially supported by The Cultivation Project Funds for Beijing University of Civil Engineering and Architecture (X23041).

#### References



- [1] Shafiee S, Topal E. When will fossil fuel reserves be diminished? *Energy Policy* 2009;37(1):181 – 9.
- [2] Sui J, Chen Z, Wang C, et al. Efficient hydrogen production from solar energy and fossil fuel via water-electrolysis and methane-steam-reforming hybridization[J]. *Applied Energy*, 2020, 276: 115409.
- [3] Chow TT. A review on photovoltaic/thermal hybrid solar technology. *Appl Energy* 2010;87:365 – 79.
- [4] Luo K, Ji J, Xu LJ, Li ZM. Seasonal experimental study of a hybrid photovoltaic water/air solar wall system. *Appl Therm Eng* 2020;169:114853.
- [5] Sajid MU, Bicer Y. Nanofluids as solar spectrum splitters: a critical review. *Sol Energy* 2020;207:974 – 1001.
- [6] Taylor R A, Otanicar T, Rosengarten G. Nanofluid-based optical filter optimization for PV/T systems[J]. *Light: Science & Applications*, 2012, 1(10): e34-e34.
- [7] Goel N, Taylor RA, Otanicar T. A review of nanofluid-based direct absorption solar collectors: design considerations and experiments with hybrid PV/Thermal and direct steam generation collectors. *Renewable Energy* 2020;145:903 – 13.
- [8] Liang H, Wang F, Yang L, et al. Progress in full spectrum solar energy utilization by spectral beam splitting hybrid PV/T system[J]. *Renewable and Sustainable Energy Reviews*, 2021, 141: 110785.
- [9] Field H. Solar cell spectral response measurement errors related to spectral band width and chopped light waveform[C]//Conference Record of the Twenty Sixth IEEE Photovoltaic Specialists Conference-1997. IEEE, 1997: 471-474.

- [10] Han X, Zhao X, Huang J, et al. Optical properties optimization of plasmonic nanofluid to enhance the performance of spectral splitting photovoltaic/thermal systems[J]. *Renewable Energy*, 2022, 188: 573-587.
- [11] Jin J, Jing D. A novel liquid optical filter based on magnetic electrolyte nanofluids for hybrid photovoltaic/thermal solar collector application[J]. *Solar Energy*, 2017, 155: 51-61.
- [12] Hjerrild N E, Crisostomo F, Chin R L, et al. Experimental results for tailored spectrum splitting metallic nanofluids for c-Si, GaAs, and Ge solar cells[J]. *IEEE Journal of Photovoltaics*, 2018, 9(2): 385-390.
- [13] Jiang W, Song J, Jia T, et al. A comprehensive review on the pre-research of nanofluids in absorption refrigeration systems[J]. *Energy Reports*, 2022, 8: 3437-3464.
- [14] Baek S, Shin D, Kim G, et al. Influence of amphoteric and anionic surfactants on stability, surface tension, and thermal conductivity of Al<sub>2</sub>O<sub>3</sub>/water nanofluids[J]. *Case Studies in Thermal Engineering*, 2021, 25: 100995.
- [15] Lowry G V, Hill R J, Harper S, et al. Guidance to improve the scientific value of zeta-potential measurements in nanoEHS[J]. *Environmental Science: Nano*, 2016, 3(5): 953-965.
- [16] Bhattacharjee S. DLS and zeta potential—what they are and what they are not?[J]. *Journal of controlled release*, 2016, 235: 337-351.
- [17] Sarafraz M M, Yang B, Pourmehran O, et al. Fluid and heat transfer characteristics of aqueous graphene nanoplatelet (GNP) nanofluid in a microchannel[J].

- International Communications in Heat and Mass Transfer, 2019, 107: 24-33.
- [18] Hordy N, Rabilloud D, Meunier J L, et al. High temperature and long-term stability of carbon nanotube nanofluids for direct absorption solar thermal collectors[J]. Solar Energy, 2014, 105: 82-90.
- [19] Tavares J, Coulombe S. Dual plasma synthesis and characterization of a stable copper–ethylene glycol nanofluid[J]. Powder technology, 2011, 210(2): 132-142.
- [20] Sani E, Mercatelli L, Barison S, et al. Potential of carbon nanohorn-based suspensions for solar thermal collectors[J]. Solar Energy Materials and Solar Cells, 2011, 95(11): 2994-3000.
- [21] Lin J, Yang H. A review on the flow instability of nanofluids[J]. Applied Mathematics and Mechanics, 2019, 40: 1227-1238.
- [22] Chang H, Tsung T T, Lin C R, et al. A study of magnetic field effect on nanofluid stability of CuO[J]. Materials Transactions, 2004, 45(4): 1375-1378.
- [23] Wang M, He L, Yin Y. Magnetic field guided colloidal assembly[J]. Materials Today, 2013, 16(4): 110-116.
- [24] Yavari M, Mansourpour Z, Shariaty-Niassar M. Controlled assembly and alignment of CNTs in ferrofluid: Application in tunable heat transfer[J]. Journal of Magnetism and Magnetic Materials, 2019, 479: 170-178.
- [25] Barai D P, Bhanvase B A, Saharan V K. Reduced graphene oxide-Fe<sub>3</sub>O<sub>4</sub> nanocomposite based nanofluids: study on ultrasonic assisted synthesis, thermal conductivity, rheology, and convective heat transfer[J]. Industrial & Engineering Chemistry Research, 2019, 58(19): 8349-8369.

- [26]Maheshwary P B, Handa C C, Nemade K R, et al. Role of nanoparticle shape in enhancing the thermal conductivity of nanofluids[J]. *Materials Today: Proceedings*, 2020, 28: 873-878.
- [27]Xian H W, Sidik N A C, Saidur R. Impact of different surfactants and ultrasonication time on the stability and thermophysical properties of hybrid nanofluids[J]. *International Communications in Heat and Mass Transfer*, 2020, 110: 104389.
- [28]Oraon A, Das B P, Michael M, et al. Impact of magnetic field on the thermal properties of chemically synthesized Sm-Co nanoparticles based silicone oil nanofluid[J]. *Journal of Thermal Analysis and Calorimetry*, 2021: 1-11.
- [29]Pourrajab R, Noghrehabadi A, Behbahani M, et al. An efficient enhancement in thermal conductivity of water-based hybrid nanofluid containing MWCNTs-COOH and Ag nanoparticles: experimental study[J]. *Journal of Thermal Analysis and Calorimetry*, 2021, 143: 3331-3343..
- [30]Wong K V, Castillo M J. Heat transfer mechanisms and clustering in nanofluids[J]. *Advances in Mechanical Engineering*, 2010, 2: 795478.
- [31]Dey D, Kumar P, Samantaray S. A review of nanofluid preparation, stability, and thermo-physical properties[J]. *Heat Transfer—Asian Research*, 2017, 46(8): 1413-1442.
- [32]Rodríguez-Laguna M R, Gómez-Romero P, Sotomayor Torres C M, et al. Modification of the Raman spectra in graphene-based nanofluids and its correlation with thermal properties[J]. *Nanomaterials*, 2019, 9(5): 804.

- [33] Das S, Giri A, Samanta S, et al. Role of graphene nanofluids on heat transfer enhancement in thermosyphon[J]. *Journal of Science: Advanced Materials and Devices*, 2019, 4(1): 163-169.
- [34] Askari S, Rashidi A, Koolivand H. Experimental investigation on the thermal performance of ultra-stable kerosene-based MWCNTs and Graphene nanofluids[J]. *International Communications in Heat and Mass Transfer*, 2019, 108: 104334..
- [35] Yang L, Ji W, Zhang Z, et al. Thermal conductivity enhancement of water by adding graphene nano-sheets: consideration of particle loading and temperature effects[J]. *International Communications in Heat and Mass Transfer*, 2019, 109: 104353.
- [36] VT P. Experimental study on the convective heat transfer performance and pressure drop of functionalized graphene nanofluids in electronics cooling system[J]. *Heat and Mass Transfer*, 2019, 55(8): 2221-2234.
- [37] Cui W, Cao Z, Li X, et al. Experimental investigation and artificial intelligent estimation of thermal conductivity of nanofluids with different nanoparticles shapes[J]. *Powder Technology*, 2022, 398: 117078.
- [38] Liao J, Zhang A, Qing S, et al. Investigation on the aggregation structure of nanoparticle on the thermal conductivity of nanofluids by molecular dynamic simulations[J]. *Powder Technology*, 2022, 395: 584-591.
- [39] Bioucas F E B, Köhn C, Jean-Fulcrand A, et al. Effective Thermal Conductivity of Nanofluids Containing Silicon Dioxide or Zirconium Dioxide Nanoparticles Dispersed in a Mixture of Water and Glycerol[J]. *International Journal of Thermophysics*, 2022, 43(11): 1-18.

- [40] Mukherjee S, Mishra P C, Chakrabarty S, et al. Effects of sonication period on colloidal stability and thermal conductivity of SiO<sub>2</sub>–water nanofluid: An experimental investigation[J]. *Journal of Cluster Science*, 2022, 33(4): 1763-1771.
- [41] Chen W, Zhai Y, Guo W, et al. A molecular dynamic simulation of the influence of linear aggregations on heat flux direction on the thermal conductivity of nanofluids[J]. *Powder Technology*, 2023, 413: 118052.
- [42] Trong Tam N, Viet Phuong N, Hong Khoi P, et al. Carbon nanomaterial-based nanofluids for direct thermal solar absorption[J]. *Nanomaterials*, 2020, 10(6): 1199.
- [43] Hulst H C, van de Hulst H C. *Light scattering by small particles*[M]. Courier Corporation, 1981.
- [44] Tien C L. *Thermal radiation in packed and fluidized beds*[J]. 1988.
- [45] Howell J R, Mengüç M P, Daun K, et al. *Thermal radiation heat transfer*[M]. CRC press, 2020..
- [46] Duan, H., Tang, L., Zheng, Y., 2017. Optical properties of hybrid plasmonic nanofluid based on core/shell nanoparticles. *Phys. E Low-Dimensional Syst. Nanostructures* 91, 88–92.
- [47] Liang, H.X., Cheng, Z.M., Wang, H., Tan, J., Wang, F., 2019. Investigation on optical properties and solar energy conversion efficiency of spectral splitting PV/T system. *Energy Procedia* 158, 15–20.
- [48] Shah J, Kumar S, Ranjan M, et al. The effect of filler geometry on thermo-optical and rheological properties of CuO nanofluid[J]. *Journal of Molecular Liquids*, 2018, 272: 668-675.

- [49] Hjerrild NE, Mesgari S, Crisostomo F, Scott JA, Amal R, Taylor RA. Hybrid PV/T enhancement using selectively absorbing Ag-SiO<sub>2</sub>/carbon nanofluids. *Sol Energy Mater Sol Cells* 2016;147:281 - 7.
- [50] Huaxu, L., Fuqiang, W., Dong, Z., Ziming, C., Chuanxin, Z., Bo, L., Huijin, X., 2020. Experimental investigation of cost-effective ZnO nanofluid based spectral splitting CPV/T system. *Energy* 194, 116913.
- [51] Tong, Y., Boldoo, T., Ham, J., Cho, H., 2020. Improvement of photo-thermal energy conversion performance of MWCNT/Fe<sub>3</sub>O<sub>4</sub> hybrid nanofluid compared to Fe<sub>3</sub>O<sub>4</sub> nanofluid. *Energy* 196, 117086.
- [52] Sajid M U, Bicer Y. Impacts of ultrasonication time and surfactants on stability and optical properties of CuO, Fe<sub>3</sub>O<sub>4</sub>, and CNTs/water nanofluids for spectrum selective applications[J]. *Ultrasonics Sonochemistry*, 2022, 88: 106079.
- [53] Han X, Chen X, Wang Q, et al. Investigation of CoSO<sub>4</sub>-based Ag nanofluids as spectral beam splitters for hybrid PV/T applications[J]. *Solar Energy*, 2019, 177: 387-394.
- [54] Han X, Chen X, Sun Y, et al. Performance improvement of a PV/T system utilizing Ag/CoSO<sub>4</sub>-propylene glycol nanofluid optical filter[J]. *Energy*, 2020, 192: 116611.
- [55] Abdelrazik A S, Al-Sulaiman F A, Saidur R. Optical behavior of a water/silver nanofluid and their influence on the performance of a photovoltaic-thermal collector[J]. *Solar Energy Materials and Solar Cells*, 2019, 201: 110054.
- [56] Abdelrazik A S, Saidur R, Al-Sulaiman F A. Investigation of the performance of a hybrid PV/thermal system using water/silver nanofluid-based optical filter[J].

Energy, 2021, 215: 119172.

- [57] Saroha S, Mittal T, Modi P J, et al. Theoretical analysis and testing of nanofluid-based solar photovoltaic/thermal hybrid collector[J]. Journal of Heat Transfer, 2015, 137(9).
- [58] An W, Chen L, Liu T, et al. Enhanced solar distillation by nanofluid-based spectral splitting PV/T technique: Preliminary experiment[J]. Solar Energy, 2018, 176: 146-156.
- [59] Abd El-Samie M M, Ju X, Xu C, et al. Numerical study of a photovoltaic/thermal hybrid system with nanofluid based spectral beam filters[J]. Energy Conversion and Management, 2018, 174: 686-704.
- [60] Zhu Q, Cui Y, Mu L, et al. Characterization of thermal radiative properties of nanofluids for selective absorption of solar radiation[J]. International journal of thermophysics, 2013, 34(12): 2307-2321.
- [61] Huaxu L, Fuqiang W, Dong L, et al. Optical properties and transmittances of ZnO-containing nanofluids in spectral splitting photovoltaic/thermal systems[J]. International Journal of Heat and Mass Transfer, 2019, 128: 668-678.
- [62] Liu Y, Dong S, Liu Y, et al. Experimental investigation on optimal nanofluid-based PV/T system[J]. Journal of Photonics for Energy, 2019, 9(2): 027501.
- [63] Ju X, Abd El-Samie M M, Xu C, et al. A fully coupled numerical simulation of a hybrid concentrated photovoltaic/thermal system that employs a therminol VP-1 based nanofluid as a spectral beam filter[J]. Applied Energy, 2020, 264: 114701.
- [64] An W, Zhang J, Zhu T, et al. Investigation on a spectral splitting



- photovoltaic/thermal hybrid system based on polypyrrole nanofluid: preliminary test[J]. *Renewable energy*, 2016, 86: 633-642.
- [65] He Y, Hu Y, Li H. An Ag@TiO<sub>2</sub>/ethylene glycol/water solution as a nanofluid-based beam splitter for photovoltaic/thermal applications in cold regions[J]. *Energy Conversion and Management*, 2019, 198: 111838.
- [66] Crisostomo F, Hjerrild N, Mesgari S, et al. A hybrid PV/T collector using spectrally selective absorbing nanofluids[J]. *Applied energy*, 2017, 193: 1-14.
- [67] Huang J, Han X, Zhao X, et al. Facile preparation of core-shell Ag@SiO<sub>2</sub> nanoparticles and their application in spectrally splitting PV/T systems[J]. *Energy*, 2021, 215: 119111.
- [68] Huang J, Han X, Zhao X, et al. The stability, optical behavior optimization of Ag@SiO<sub>2</sub> nanofluids and their application in spectral splitting photovoltaic/thermal receivers[J]. *Renewable Energy*, 2022, 190: 865-878.
- [69] Zhao X, Han X, Yao Y, et al. Stability investigation of propylene glycol-based Ag@SiO<sub>2</sub> nanofluids and their performance in spectral splitting photovoltaic/thermal systems[J]. *Energy*, 2022, 238: 122040.
- [70] Dmour A, Xiao Y, Tian W, et al. CQD-ATO hybrid nanofluid with good stability in the application of spectral beam splitters[J]. *Solar Energy Materials and Solar Cells*, 2023, 261: 112536.
- [71] Martínez-Merino P, Estellé P, Alcántara R, et al. Thermal performance of nanofluids based on tungsten disulphide nanosheets as heat transfer fluids in parabolic trough solar collectors[J]. *Solar Energy Materials and Solar Cells*, 2022,

247: 111937.

- [72] Abdelgaied M, Attia M E H, Kabeel A E, et al. Improving the thermo-economic performance of hemispherical solar distiller using copper oxide nanofluids and phase change materials: Experimental and theoretical investigation[J]. *Solar Energy Materials and Solar Cells*, 2022, 238: 111596.
- [73] Yan C, Liang J, Zhong X, et al. BN white graphene well-dispersed solar salt nanofluids with significant improved thermal properties for concentrated solar power plants[J]. *Solar Energy Materials and Solar Cells*, 2022, 245: 111875.
- [74] Farooq S, Vital C V P, Tikhonowski G, et al. Thermo-optical performance of bare laser-synthesized TiN nanofluids for direct absorption solar collector applications[J]. *Solar Energy Materials and Solar Cells*, 2023, 252: 112203.
- [75] Gao Q, Lu Y, Yu Q, et al. High-temperature corrosion behavior of austenitic stainless steel in quaternary nitrate molten salt nanofluids for concentrated solar power[J]. *Solar Energy Materials and Solar Cells*, 2022, 245: 111851.
- [76] Navarro M E, Palacios A, Jiang Z, et al. Effect of SiO<sub>2</sub> nanoparticles concentration on the corrosion behaviour of solar salt-based nanofluids for Concentrating Solar Power plants[J]. *Solar Energy Materials and Solar Cells*, 2022, 247: 111923.
- [77] Wciślik S. A simple economic and heat transfer analysis of the nanoparticles use[J]. *Chemical Papers*, 2017, 71: 2395-2401.
- [78] Said Z, Ghodbane M, Boumeddane B, et al. Energy, exergy, economic and environmental (4E) analysis of a parabolic trough solar collector using MXene based silicone oil nanofluids[J]. *Solar Energy Materials and Solar Cells*, 2022, 239:

111633.

[79]Seyyedi S M, Dogonchi A S, Hashemi-Tilehnoee M, et al. Entropy generation and economic analyses in a nanofluid filled L-shaped enclosure subjected to an oriented magnetic field[J]. Applied Thermal Engineering, 2020, 168: 114789.